differences between $OCPh_3$ and $OSiPh_3$ may arise primarily from the differing O–C and O–Si distances. With La and Ce, the longer distance in the $OSiPh_3$ complexes provides flexibility to the ligand set, which may allow metal–(arene ring) interactions to occur. Since this less congested ligand set may also allow solvents to displace the metal–arene interaction and form solvated complexes, the enhanced solubility of **3** and **4** over **1** and **2** may also result from the longer O–Si distance. Hence, $OCPh_3$ ligands may be advantageous when reduced solubility is required and vice versa for $OSiPh_3$.

Note Added in Proof. A note on the structure of the yttrium analogue of **3** and **4** has recently appeared: Coan, P. S.; McGeary, M. J.; Lobkovsky, E. B.; Caulton, K. G. *Inorg. Chem.* **1991**, *30*, 3570–3572.

Acknowledgment. For support of this research, we thank the Division of Chemical Sciences of the Office of Basic Energy Sciences of the Department of Energy. Funds for the purchase of the Nicolet R3m/V diffractometer system were made available from the National Science Foundation under Grant CHE-85-14495.

Registry No. **1** (coordination compound entry), 137465-15-7; **1** (salt entry), 137465-25-9; **1**·3PhMe, 137465-21-5; **2** (coordination compound entry), 137465-16-8; **2** (salt entry), 137465-26-0; **2**·4PhMe, 137465-23-7; **3** (coordination compound entry), 137465-17-9; **3** (salt entry), 125545-55-3; **3**·2PhMe, 137465-24-8; **4** (coordination compound entry), 137465-18-0; **4** (salt entry), 125545-52-0; **4**·2PhMe, 137465-22-6; **5** (x = 2), 137465-19-1; **5** (x = 4), 137465-28-2; **6** (x = 2), 137465-20-4; **6** (x = 4), 137465-30-6; **7**·THF, 133294-54-9; **8**·THF, 124685-78-5; $KN(SiMe_3)_2$, 40949-94-8; $LaCl_3$, 10099-58-8; $CeCl_3$, 7790-86-5; $La[N(SiMe_3)_2]_3$, 35788-99-9; $Ce[N(SiMe_3)_2]_3$, 41836-21-9.

Supplementary Material Available: Tables of crystal data, bond distances and angles, thermal parameters, and hydrogen atom coordinates for **1** and **4** and a textual description and ORTEP diagram of the disordered toluene molecule in **1** (24 pages); listings of structure factor amplitudes for **1** and **4** (65 pages). Ordering information is given on any current masthead page.

Contribution from the Koninklijke/Shell Laboratorium, Amsterdam (Shell Research B.V.), P.O. Box 3003, 1003 AA Amsterdam, The Netherlands, and School of Chemistry, University of Bristol, Bristol BS8 1TS, U.K.

Chemistry of (Octaethylporphyrinato)lutetium and -yttrium Complexes: Synthesis and Reactivity of (OEP)MX Derivatives and the Selective Activation of O_2 by (OEP)Y(μ-Me)$_2$AlMe$_2$

Colin J. Schaverien*,† and A. Guy Orpen‡

Received June 19, 1991

Reaction of ML_3 (M = Lu, Y; L = $CH(SiMe_3)_2$, O-2,6-$C_6H_3{}^tBu_2$) with octaethylporphyrin ($OEPH_2$) affords (OEP)ML complexes [M = Lu (**1a**), Y (**1b**), L = $CH(SiMe_3)_2$; M = Lu (**2a**), Y (**2b**), L = O-2,6-$C_6H_3{}^tBu_2$]. The crystal structure of (OEP)LuCH-$(SiMe_3)_2$ (**1a**) shows a highly dished porphyrin skeleton with the square-pyramidal, five-coordinate lutetium atom 0.918 Å out of the N_4 plane of the porphyrin ligand. Crystal data: monoclinic, $P2_1/c$, a = 14.879 (6) Å, b = 20.644 (10) Å, c = 14.161 (5) Å, β = 96.38 (3)°, Z = 4, T = 200 K, and R = 0.045 (4098 reflections with $I \geq 2\sigma(I)$). Alkyl species **1** undergo facile protonolysis with HO-2,6-$C_6H_3{}^tBu_2$, HCC^{t}Bu, or H_2O to give monomeric alkoxide, dimeric alkynyl, and dimeric hydroxide species $[(OEP)MX]_n$ (n = 1, 2) [M = Lu, Y; X = O-2,6-$C_6H_3{}^tBu_2$ (**2a,b**), CC^{t}Bu (**3a,b**), OH (**4a,b**)], respectively. Titration of (OEP)M(μ-OH)$_2$M-(OEP) (**4**) with H_2O affords water adducts (OEP)M(μ-OH)$_2$(H_2O)$_x$M(OEP). A synthetically more convenient route to **1** is via reaction of **2** with $LiCH(SiMe_3)_2$. In marked contrast to the facile hydrogenation of $Ln(C_5Me_5)_2CH(SiMe_3)_2$, alkyl species **1** do not undergo σ-bond metathesis with H_2 (20 atm, 25 °C, C_6D_{12}). Reaction of (OEP)Y$OC_6H_3{}^tBu_2$ (**2b**) with MeLi (2 equiv) in ether affords ether-insoluble (OEP)Y(μ-Me)$_2$Li(OEt_2) (**5**). Treatment with $AlMe_3$ (2 equiv) in hexane yields monomeric, highly fluxional (OEP)Y(μ-Me)$_2$AlMe$_2$ (**6**), which selectively activates O_2 to afford (OEP)Y(μ-OMe)$_2$AlMe$_2$ (**7**). Comparison of the reactivity of these species, particularly **1** and **6**, with their C_5H_5 and C_5Me_5 counterparts is described. ^{17}O NMR data on labeled **4a**, **4b**, and **7** are presented and discussed.

Introduction

Porphyrin complexes of the late transition metals have attracted considerable attention as models for cytochrome P450 and as olefin oxidation catalysts.[1] In contrast, the chemistry of aluminum,[2] early transition metal,[3] lanthanide,[4] or actinide[5] species supported by a porphyrin ligand has been less well studied. Despite the range of metals for which porphyrin complexes are known, there are no examples which possess a lanthanide–carbon σ bond. Previous preparations of porphyrin complexes have frequently employed synthetic methods seemingly incompatible with the preparation of very hydrolytically sensitive species, involving heating the components in an imidazole melt or refluxing in 1,2,4-trichlorobenzene, followed by chromatography on alumina.

As part of our investigation of different ligand types capable of supporting lanthanide *alkyl* complexes, we rationalized that a porphyrin ligand would provide an alternative and acceptable coordination environment in organolanthanide chemistry and that the pendant porphyrin alkyl groups would provide sufficient steric protection and hydrocarbon solubility. The constraint of other attendant ligands to a mutually trans geometry by the porphyrin framework and the corresponding inhibition of cis coordination necessary[6] for β-hydride elimination and olefin insertion reactions[7]

Table I. Crystal Data and Data Collection Parameters for **1a**[a]

chem formula	$C_{43}H_{63}LuN_4Si_2$
mol wt	867.12
space group	$P2_1/c$ (No. 14)
a, Å	14.879 (6)
b, Å	20.644 (10)
c, Å	14.161 (5)
β, deg	96.38 (3)
V, Å^3	4323 (3)
Z	4
D_{calcd}, g cm^{-3}	1.33
μ(Mo Kα) cm^{-1}	23.7
λ, Å	0.71069
T, K	200
no. of obsd refcns, $I > 2\sigma(I)$	4098
R	0.045 (0.071 using all 5675 unique data)
R_w	0.043 (0.051 using all 5675 unique data)
goodness of fit; no. of params	1.154; 464

[a] $R = \sum|\Delta|/\sum|F_o|$; $R_w = [\sum w\Delta^2/\sum wF_o^2]^{1/2}$; $S = [\sum w\Delta^2/(NO - NV)]^{1/2}$; $\Delta = F_o - F_c$.

† Koninklijke/Shell Laboratorium, Amsterdam.
‡ University of Bristol.

0020-1669/91/1330-4968$02.50/0

Table II. Atomic Coordinates (×10⁴) and Isotropic Thermal Parameters (Å² × 10³) for **1a**

	x	*y*	*z*	*U*[a]
Lu	2372 (1)	824 (1)	1943 (1)	28 (1)
Si(1)	1825 (2)	−122 (1)	3962 (2)	49 (1)
Si(2)	3479 (2)	−556 (1)	2896 (2)	46 (1)
N(1)	2343 (4)	1702 (3)	2864 (4)	34 (2)
N(2)	3759 (4)	1223 (3)	1792 (4)	33 (2)
N(3)	2401 (4)	717 (3)	332 (5)	35 (2)
N(4)	967 (4)	1181 (3)	1443 (5)	33 (2)
C(1)	2378 (6)	−143 (4)	2849 (6)	37 (3)
C(2)	1579 (5)	1946 (4)	3218 (6)	35 (3)
C(3)	1838 (6)	2310 (4)	4069 (6)	37 (3)
C(4)	2763 (6)	2298 (4)	4217 (6)	42 (3)
C(5)	3069 (5)	1923 (4)	3456 (6)	33 (3)
C(6)	3947 (5)	1848 (4)	3268 (6)	37 (3)
C(7)	4282 (5)	1543 (4)	2504 (6)	35 (3)
C(8)	5210 (5)	1578 (4)	2290 (6)	35 (3)
C(9)	5232 (5)	1288 (4)	1438 (6)	35 (3)
C(10)	4327 (5)	1058 (4)	1129 (6)	33 (3)
C(11)	4028 (5)	775 (4)	252 (5)	34 (3)
C(12)	3156 (5)	631 (3)	−125 (5)	27 (3)
C(13)	2880 (6)	453 (4)	−1104 (6)	35 (3)
C(14)	1952 (6)	412 (4)	−1215 (6)	39 (3)
C(15)	1665 (5)	597 (4)	−308 (6)	31 (3)
C(16)	771 (5)	688 (4)	−135 (6)	38 (3)
C(17)	431 (5)	972 (4)	631 (6)	35 (3)
C(18)	−495 (5)	1176 (5)	680 (7)	42 (3)
C(19)	−514 (6)	1509 (5)	1492 (7)	50 (4)
C(20)	403 (6)	1524 (5)	1966 (7)	46 (4)
C(21)	699 (6)	1862 (5)	2786 (7)	46 (4)
C(22)	1209 (6)	2613 (5)	4685 (7)	55 (4)
C(23)	824 (8)	2123 (5)	5354 (8)	83 (5)
C(24)	3361 (6)	2600 (4)	5009 (6)	44 (3)
C(25)	3707 (8)	2111 (5)	5758 (7)	77 (5)
C(26)	5969 (6)	1908 (5)	2898 (6)	52 (4)
C(27)	6347 (7)	1461 (6)	3712 (8)	91 (6)
C(28)	6017 (5)	1244 (5)	855 (6)	45 (3)
C(29)	6113 (6)	1851 (5)	263 (7)	54 (4)
C(30)	3504 (6)	387 (5)	−1845 (6)	50 (4)
C(31)	3710 (7)	1053 (5)	−2251 (8)	77 (5)
C(32)	1334 (7)	316 (5)	−2111 (6)	55 (4)
C(33)	1000 (7)	946 (5)	−2572 (7)	78 (5)
C(34)	−1268 (5)	1075 (5)	−96 (7)	52 (4)
C(35)	−1352 (7)	1625 (5)	−805 (7)	72 (5)
C(36)	−1301 (7)	1844 (9)	1882 (9)	80 (6)
C(37A)	−1574 (11)	1609 (11)	2686 (15)	71 (10)
C(37B)	−1472 (15)	2407 (14)	1728 (19)	77 (12)
C(38)	1523 (8)	−943 (5)	4402 (9)	90 (6)
C(39)	720 (6)	313 (5)	3805 (8)	67 (4)
C(40)	2531 (8)	301 (7)	4941 (7)	94 (6)
C(41)	3775 (6)	−671 (5)	1663 (6)	56 (4)
C(42)	3552 (8)	−1388 (5)	3420 (8)	79 (5)
C(43)	4401 (6)	−92 (5)	3567 (8)	72 (5)

[a] Equivalent isotropic *U* defined as one-third of the trace of the orthogonalized U_{ij} tensor.

could lead to new reaction pathways. Some of the results reported herein have appeared in preliminary form.[8]

Scheme I

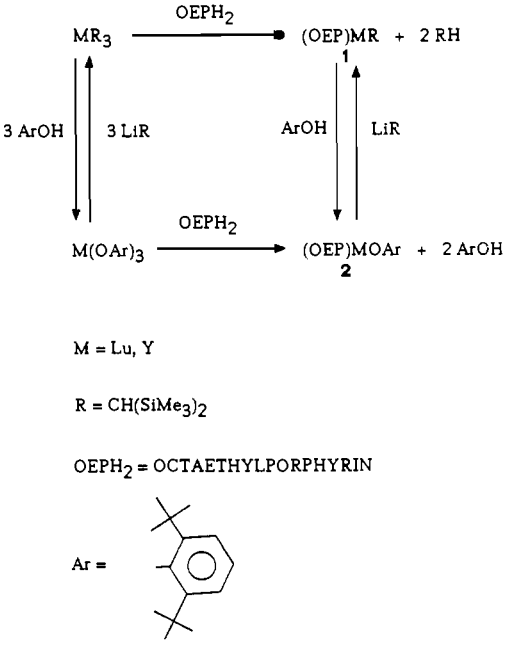

Scheme II

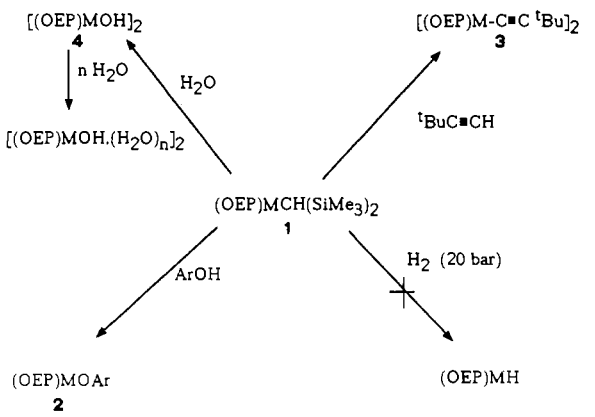

Table III. Selected Bond Lengths (Å) for **1a**

Lu–N(1)	2.236 (7)	Lu–C(1)	2.374 (8)
Lu–N(2)	2.253 (6)	Si(1)–C(1)	1.856 (9)
Lu–N(3)	2.296 (7)	Si(2)–C(1)	1.842 (9)
Lu–N(4)	2.256 (6)		

Table IV. Selected Bond Angles (deg) for **1a**

N(1)–Lu–N(2)	80.6 (2)	N(2)–Lu–C(1)	114.2 (3)
N(1)–Lu–N(3)	131.4 (2)	N(3)–Lu–C(1)	117.2 (3)
N(2)–Lu–N(3)	79.8 (2)	N(4)–Lu–C(1)	113.0 (3)
N(1)–Lu–N(4)	80.9 (2)	Si(1)–C(1)–Si(2)	117.2 (4)
N(2)–Lu–N(4)	132.7 (2)	Lu–C(1)–Si(1)	117.7 (4)
N(3)–Lu–N(4)	80.7 (2)	Lu–C(1)–Si(2)	111.0 (4)
N(1)–Lu–C(1)	114.4 (3)		

Table V. Displacements (Å) of Metals out of the N_4 Mean Plane

compd	M–porphyrin N_4 mean plane	ref
$(OEP)LuCH(SiMe_3)_2$	0.918	this work
$(TPP)UCl_2(THF)$	1.29	5a
$Ce(OEP)_2$	1.376	4c
$Ce_2(OEP)_3$	1.394, 1.876	4c
$Nd_2(Pc)_2(TMPP)$[a]	1.29	4b
(OEP)ScCl	0.68	3a
$[(TTP)Sc]_2(\mu\text{-}O)$	0.82	3a
$(OEP)Sc(C_5H_5)$	0.80	3b

[a] TMPP = tetrakis(4-methoxyphenyl)porphyrin; Pc = phthalocyanine.

(1) (a) Collman, J. P.; Hegedus, L. S.; Norton, J. R.; Finke, R. G. *Principles and Applications of Organotransition Metal Chemistry*; University Science Books: Mill Valley, CA, 1987; pp 182. (b) Valentine, J. S.; Burstyn, J. N.; Margerum, L. D. *Oxygen Complexes and Oxygen Activation by Transition Metals*; Martell, A. E., Sawyer, D. T., Eds.; Plenum Press: New York, 1988; pp 175. (c) Hay, R. W. *Bioinorganic Chemistry*; Ellis Horwood Books: London, 1984. (d) Groves, J. T. *J. Chem. Educ.* **1985**, *62*, 928. (e) White, R. E.; Coone, M. J. *Annu. Rev. Biochem.* **1980**, *49*, 315. (f) Groves, J. T. *Adv. Inorg. Biochem.* **1979**, 119. (g) Brothers, P. J.; Collman, J. P. *Acc. Chem. Res.* **1986**, *19*, 209. (h) Collman, J. P.; Brauman, J. I.; Meunier, B.; Raybuck, S. A.; Kodadek, T. *Proc. Natl. Acad. Sci. U.S.A.* **1984**, *81*, 3245. (i) Collman, J. P.; Kodadek, T.; Raybuck, S.; Brauman, J. I.; Papazian, L. M. *J. Am. Chem. Soc.* **1985**, *107*, 4343. (j) Groves, J. T.; Nemo, T. E. *J. Am. Chem. Soc.* **1983**, *105*, 5786. (k) Collman, J. P.; Halbert, T. R.; Suslick, K. S. In *Metal Ion Activation of Dioxygen*; Spiro, T. G., Ed.; Wiley: New York, 1980.

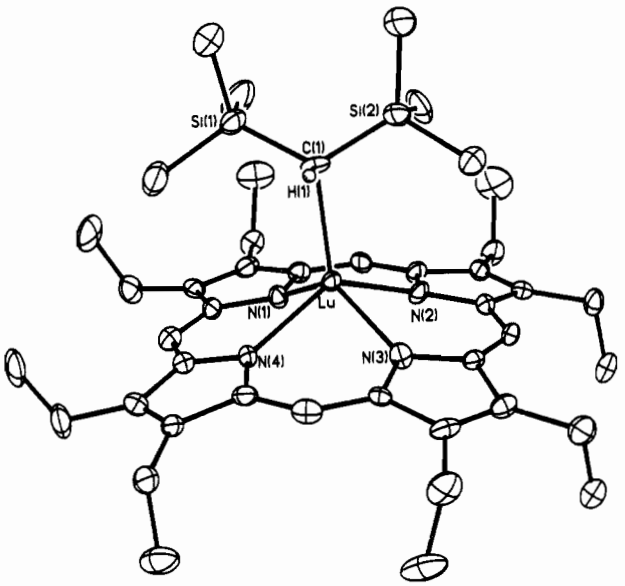

Figure 1. Molecular structure of **1a**. Non-hydrogen atoms are represented by ellipsoids enclosing 30% probability density. Ethyl and methyl group hydrogens have been omitted for clarity.

Results

Reaction of ML_3 (M = Lu, Y; L = $CH(SiMe_3)_2$, O-2,6-$C_6H_3{}^tBu_2$) with octaethylporphyrin ($OEPH_2$) in toluene afforded purple (OEP)ML complexes [M = Lu (**1a**), Y, (**1b**), L = $CH(SiMe_3)_2$; M = Lu (**2a**), Y (**2b**), L = O-2,6-$C_6H_3{}^tBu_2$] in good to excellent yield. These results are summarized in Scheme I.

The crystal structure of $(OEP)LuCH(SiMe_3)_2$ (**1a**) was determined and shows a highly dished porphyrin skeleton with the square-pyramidal, five-coordinate lutetium atom 0.918 Å out of the N_4 plane of the porphyrin ligand. Perspective views of **1a** are shown in Figures 1 and 2. Details of crystal data and structure analysis are given in Table I. Atomic coordinates, selected bond lengths, and selected bond angles are listed in Tables II–IV, respectively.

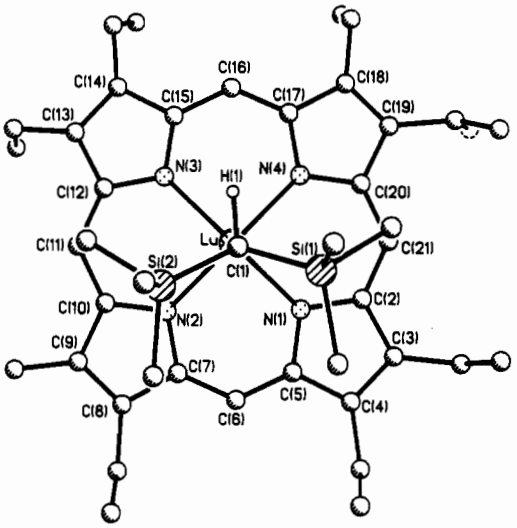

Figure 2. Molecular structure **1a** viewed perpendicular to the porphyrin N_4 plane. Ethyl and methyl group hydrogens have been omitted for clarity.

Scheme III

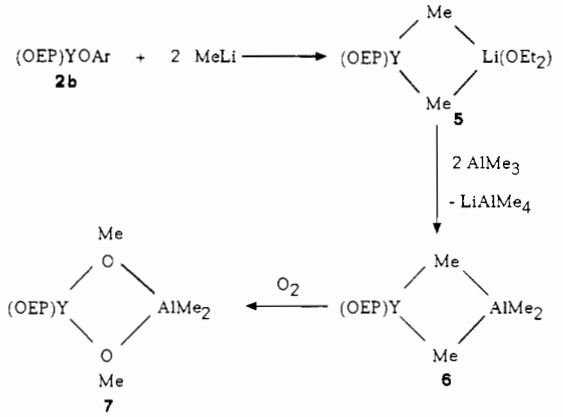

Alkyl species **1** undergo facile protonolysis with HO-2,6-$C_6H_3{}^tBu_2$, HCC^{t}Bu, or H_2O to give monomeric alkoxide, dimeric alkynyl, and dimeric hydroxide species $[(OEP)MX]_n$ (n = 1, 2) [M = Lu, Y; X = O-2,6-$C_6H_3{}^tBu_2$ (**2a,b**), X = CC^{t}Bu (**3a,b**), X = OH, (**4a,b**)], respectively. See Scheme II. Titration of $(OEP)M(\mu\text{-}OH)_2M(OEP)$ (**4**) with H_2O affords water adducts $(OEP)M(\mu\text{-}OH)_2(H_2O)_xM(OEP)$. Exchange reactions between free and coordinated water and incorporation of ^{17}O into the μ-OH site have been investigated using ^{17}O NMR spectroscopy. ^{17}O NMR data on the ^{17}O enriched complexes **4a**, δ 96 ppm, and **4b**, δ 100 ppm, are also reported.

Reaction of $(OEP)YOC_6H_3{}^tBu_2$ (**2b**) with MeLi (2 equiv) in ether affords ether-insoluble $(OEP)Y(\mu\text{-}Me)_2Li(OEt_2)$ (**5**), which, on treatment with $AlMe_3$ (2 equiv) in hexane, yields monomeric, highly fluxional $(OEP)Y(\mu\text{-}Me)_2AlMe_2$ (**6**), which selectively activates O_2 to afford $(OEP)Y(\mu\text{-}OMe)_2AlMe_2$ (**7**). Labeling studies with $^{17}O_2$ confirm this incorporation mode. These results are summarized in Scheme III.

Discussion

In order to circumvent a stepwise alkylation sequence, or the use of high-boiling solvents, reaction of a porphyrin (PH_2) with a homoleptic lanthanide tris(alkyl) LnR_3 (Ln = a lanthanide metal) allows protonolysis under mild conditions, thereby avoiding salt or donor-solvent coordination.[9] Furthermore, an advantage

(2) (a) Inoue, S.; Takeda, N. *Bull. Chem. Soc. Jpn.* **1977**, *50*, 984. (b) Kuroki, M.; Aida, T.; Inoue, S. *J. Am. Chem. Soc.* **1987**, *109*, 4737. (c) Aria, T.; Murayama, H.; Inoue, S. *J. Org. Chem.* **1989**, *54*, 414. (d) Yasida, T.; Aida, T.; Inoue, S. *Bull. Chem. Soc. Jpn.* **1986**, *59*, 3931.
(3) (a) Sewchok, M. G.; Haushalter, R. C.; Merola, J. S. *Inorg. Chim. Acta* **1988**, *144*, 47. (b) Arnold, J.; Hoffman, C. G. *J. Am. Chem. Soc.* **1990**, *112*, 8621. (c) Marchon, J.; Latour, J.; Grand, A.; Belakhovsky, M.; Loos, M.; Goulon, J. *Inorg. Chem.* **1990**, *29*, 57. (d) Buchler, J. W.; Folz, M.; Habets, H.; Van Kaam, J.; Rohbock, K. *Chem. Ber.* **1976**, *109*, 1477.
(4) (a) Srivastava, T. S. *Bioinorg. Chem.* **1978**, *8*, 61. (b) Moussavi, M.; De Cian, A.; Fischer, J.; Weiss, R. *Inorg. Chem.* **1986**, *25*, 2107. (c) Buchler, J. W.; De Cian, A.; Fischer, J.; Kihn-Botulinski, M.; Paulus, H.; Weiss, R. *J. Am. Chem. Soc.* **1986**, *108*, 3652. (d) Donohoe, R. J.; Duchowski, J. K.; Bocian, D. F. *J. Am. Chem. Soc.* **1988**, *110*, 6119. (e) Horrocks, W. D., Jr.; Wong, C.-P. *J. Am. Chem. Soc.* **1976**, *98*, 7157. (f) Wong, C.-P. *Inorg. Synth.* **1983**, *22*, 156. (g) Buchler, J. W.; De Cian, A.; Fischer, J.; Kihn-Botulinski, M.; Weiss, R. *Inorg. Chem.* **1988**, *27*, 339. (h) Buchler, J. W.; Hüttermann, J.; Löffler, J. *Bull. Chem. Soc. Jpn.* **1988**, *61*, 71. (i) Buchler, J. W.; Kihn-Botulinski, M.; Scharbert, B. *Z. Naturforsch.* **1988**, *43B*, 1371. (j) Buchler, J. W.; Scharbert, B. *J. Am. Chem. Soc.* **1988**, *110*, 4272 and references therein.
(5) (a) Girolami, G.; Milan, S. N.; Suslick, K. S. *Inorg. Chem.* **1987**, *26*, 343 and references therein. (b) Dormomd, A.; Belkalem, B.; Charpon, P.; Lance, M.; Vigner, D.; Folcher, G.; Guilard, R. *Inorg. Chem.* **1986**, *25*, 4785. (c) Wong, C.-P.; Horrocks, W. D., Jr. *Tetrahedron Lett.* **1975**, *31*, 2637.
(6) (a) Doherty, N. M.; Bercaw, J. E. *J. Am. Chem. Soc.* **1985**, *107*, 2670. (b) In $[PtH(C_2H_4)(PEt_3)_2]^+$ [6b] and $IrH(C_2H_4)(CO)(Cl)(PPh_3)_2$ [6c] the mutually trans orientation of the hydride and olefin inhibits intramolecular insertion of the olefin. Inhibition of CO insertion into a macrocycle-supported Rh–Et bond has been reported.[6d] (b) Deeming, A. J.; Johnson, B. F. G.; Lewis, J. *J. Chem. Soc., Dalton Trans.* **1973**, 1848. (c) Olgemöller, B.; Beck, W. *Angew. Chem., Int. Ed. Engl.* **1980**, *19*, 834. (d) Reference 1a, p 375.
(7) (a) Burger, B. J.; Thompson, M. E.; Cotter, W. D.; Bercaw, J. E. *J. Am. Chem. Soc.* **1990**, *112*, 1566. (b) Steigerwald, M. L.; Goddard, W. A., III. *J. Am. Chem. Soc.* **1984**, *106*, 308. (c) Rabaâ, H.; Saillard, J.-Y.; Hoffmann, R. *J. Am. Chem. Soc.* **1986**, *108*, 4327.
(8) Schaverien, C. J. *J. Chem. Soc., Chem. Commun.* **1991**, 458.
(9) Schumann, H. *Fundamental and Technological Aspects of Organo-f-Element Chemistry*; Marks, T. J.; Fragalà, I. L., Eds.; NATO ASI Series; D. Reidel: Boston, MA, 1985; p 1.

Scheme IV

$LuR_3 + TTPH_2 \not\longrightarrow (TTP)LuR$

$LuR_3 + TMPH_2 \not\longrightarrow (TMP)LuR$

$LaR_3 + OEPH_2 \not\longrightarrow (OEP)LaR$

$La(OAr)_3 + OEPH_2 \not\longrightarrow (OEP)LaOAr$

$R = CH(SiMe_3)_2$ OAr =

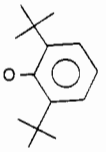

$TTPH_2$ = tetratolylporphyrin

$TMPH_2$ = tetramesitylporphyrin

$OEPH_2$ = octaethylporphyrin

of this new approach is that it has potential generality in the porphyrin ligand, and a range of lanthanide tris(alkyls) $Ln\{CH(SiMe_3)_2\}_3$ (Ln = Y,[10a] La,[10b] Sm,[10b] Lu[10a]) are known.

$$LnR_3 + PH_2 \rightarrow (P)LnR + 2RH$$

Reaction of $M\{CH(SiMe_3)_2\}_3$ (M = Lu, Y)[10a] with octaethylporphyrin ($OEPH_2$) in benzene or toluene (60 °C, 6 h) affords purple, hexane-soluble $(OEP)MCH(SiMe_3)_2$ [M = Lu (**1a**), Y (**1b**)] in 70–80% isolated yield, with accompanying loss of $CH_2(SiMe_3)_2$. See Scheme I.

The ethyl protons give rise to an ABX_3 multiplet [J_{AB} = 17 Hz, $J_{AX} = J_{BX}$ = 7.6 Hz (simulated)], consistent with the nonequivalence of the two sides of the porphyrin ring. Although the methylene protons of (OEP)MX complexes are per se diastereotopic, their magnetic nonequivalence is enhanced by the out-of-plane position of the metal and by a correlated rotation of neighboring ethyl groups.[11] The difference between the chemical shifts of the methylene protons $\delta_A - \delta_B$ in these, and almost[12] all other (OEP)M complexes herein, remains small (ca. 0.05 ppm), indicating that although the metal resides out of the porphyrin plane, little inequivalence between the two porphyrin faces is induced. The ^1H NMR resonances of the $CH(SiMe_3)_2$ ligand are isotropically shifted due to the ring current of the porphyrin ring with the $SiMe_3$ and α-CH groups resonating at −1.76 and −5.78 ppm (M = Lu), respectively. For M = Y, the corresponding chemical shifts are −1.78 and −5.33 ppm (J_{YH} = 2.5 Hz), respectively. The methyne group resonates at 41.05 ppm [$^1J(C_\alpha H)$ = 95 Hz] (M = Lu). The inherently greater chemical shift dispersion in ^{13}C NMR spectroscopy means that the porphyrin-induced isotropic shift is less pronounced, although possibly of a similar magnitude to that observed in the ^1H NMR spectrum.

Although sandwichlike octaethylporphyrin complexes $Ln(OEP)_2$ of all the lanthanides[4c,g-j] (except Pm) are known, and tetraphenylporphyrin complexes $(TPP)Ln(acac)$[4f] (Ln = La–Lu, except Pm) have also been prepared, no such complexes containing an alkyl group have yet been reported. However, in the chemistry described here, the propensity to form (porphyrin)lanthanide alkyl species is highly dependent on both the nature of the porphyrin and the lanthanide metal. For example, in contrast to the ease of incorporation of octaethylporphyrin into the lutetium and yttrium coordination sphere, reaction of $La\{CH(SiMe_3)_2\}_3$[10b] with $OEPH_2$ results in the rapid appearance of $CH_2(SiMe_3)_2$ by ^1H NMR spectroscopy, but no porphyrin alkyl complex could be identified, neither by ^1H NMR monitoring of the reaction carried out in C_6D_6 nor in the isolated product mixture. Reaction of $Lu\{CH(SiMe_3)_2\}_3$ with tetratolylporphyrin ($TTPH_2$) or sterically more protecting tetramesitylporphyrin ($TMPH_2$) did not give either $(TTP)LuCH(SiMe_3)_2$ or $(TMP)LuCH(SiMe_3)_2$ (Scheme IV).

To confirm the lutetium coordination in the first porphyrin lanthanide alkyl complex, and the porphyrin-induced effects on $CH(SiMe_3)_2$ geometry, the molecular structure of $(OEP)LuCH(SiMe_3)_2$ (**1a**) was determined by single-crystal X-ray diffraction methods. The coordination geometry at lutetium is approximately square pyramidal with the apical site occupied by the $CH(SiMe_3)_2$ group and the basal sites by the octaethylporphyrin nitrogen atoms (Figures 1 and 2). The lutetium atom lies 0.918 Å above the mean plane of the four pyrrole nitrogen atoms to which it is essentially equidistantly bonded [Lu–N(1) = 2.236 (7), Lu–N(2) = 2.253 (6), Lu–N(3) = 2.296 (7), Lu–N(4) = 2.256 (6) Å]. The N_4C_{20} core of the porphyrin unit best resembles a C_{4v} saucer with mean deviations of the nitrogens, pyrrole α-carbons, and pyrrole β-carbons [C(3), C(4), C(8), C(9), C(13), C(14), C(18), C(19)] out of the N_4 mean plane being 0.014, 0.157 (22), and 0.396 (48) Å, respectively. The mean deviation of C(6), C(11), C(16), and C(21) is 0.203 (41) Å. The saucering is not perfectly symmetrical, the distortion being least for C(5)–C(7). The Lu–C_α bond length of 2.374 (8) Å is similar to that observed for other Lu–C σ bonds.[14] The Lu–N distances are similar to those found in other lanthanide–nitrogen donor complexes,[15] after taking into consideration differences in ionic radii.[13] In contrast to the geometry found in $Ln(C_5Me_5)_2CH(SiMe_3)_2$,[16] the bis(trimethylsilyl)methyl ligand is not significantly distorted or asymmetrically bonded [Lu–C(1)–Si(1) = 117.7 (4), Lu–C(1)–Si(2) = 111.0 (4)°]. There is no interaction of the lutetium atom with any of the methyl groups, and the calculated Lu···H(1) distance is quite long at 2.74 (10) Å. The X-ray structure determination does not therefore support an agostic interaction with the lutetium atom [Lu–C(1)–H(1) =

(10) (a) $Y\{CH(SiMe_3)_2\}_3$ and $Lu\{CH(SiMe_3)_2\}_3$ were prepared by analogy to $Ln\{CH(SiMe_3)_2\}_3$ (Ln = Sm, La):[10b] see Experimental Section. (b) Hitchcock, P. B.; Lappert, M. F.; Smith, R. G.; Barlett, R. G.; Power, P. P. *J. Chem. Soc., Chem. Commun.* **1988**, 1007.

(11) Abraham, R. J.; Smith, K. M. *Tetrahedron Lett.* **1971**, 3335.

(12) The exception is $(OEP)LuCH(SiMe_3)_2(\mu\text{-Cl})K$ (**1a**·KCl) (see Experimental Section) where $\delta_A - \delta_B$ = 0.43 ppm, presumably indicative of axially coordinated KCl, trans to $CH(SiMe_3)_2$ in six-coordinate **1a**·KCl. A full description of the synthesis, reactivity, and X-ray structure of $Lu\{CH(SiMe_3)_2\}_3(\mu\text{-Cl})K(\eta^6\text{-toluene})_2$ and the synthesis of $Lu\{CH(SiMe_3)_2\}_3(\mu\text{-Cl})K$ can be found in: Schaverien, C. J.; Van Mechelen, J. B. *Organometallics* **1991**, *10*, 1704. We assume that the KCl coordination mode in $(OEP)LuCH(SiMe_3)_2(\mu\text{-Cl})K$ is similar to that found in $Lu\{CH(SiMe_3)_2\}_3(\mu\text{-Cl})K(\eta^6\text{-toluene})_2$. See also: Schaverien, C. J.; Nesbitt, G. J. *J. Chem. Soc., Dalton Trans.*, in press.

(13) Shannon, R. D. *Acta Crystallogr., Sect. A* **1976**, *32*, 751.

(14) (a) Van der Heijden, H.; Pasman, P.; De Boer, E. J. M.; Schaverien, C. J.; Orpen, A. G. *Organometallics* **1989**, *8*, 1459. (b) Schumann, H.; Genthe, W.; Bruncks, N.; Pickardt, J. *Organometallics* **1982**, *1*, 1194. (c) Schumann, H.; Albrecht, I.; Reier, F.-W.; Hahn, E. *Angew. Chem., Int. Ed. Engl.* **1984**, *23*, 522. (d) Evans, W. J.; Wayda, A. L.; Hunter, W. E.; Atwood, J. L. *J. Chem. Soc., Chem. Commun.* **1981**, 292. (e) Schumann, H.; Lauke, H.; Hahn, E.; Pickardt, J. *J. Organomet. Chem.* **1984**, *263*, 29. (f) Cotton, S. A.; Hart, F. A.; Hursthouse, M. B.; Welch, A. J. *J. Chem. Soc., Chem. Commun.* **1972**, 1225. (g) Schumann, H.; Albrecht, I.; Hahn, E. *J. Organomet. Chem.* **1984**, *276*, C5. (h) Watson, P. L.; Parshall, G. *Acc. Chem. Res.* **1985**, *18*, 51.

(15) In $Ho(NMeCH_2CH_2NMe_2)_2Li(NMeCH_2CH_2NMe_2)_2$, Ho–NMe = 2.279 Å whereas dative Ho–NMe_2 = 2.662 Å: Schumann, H.; Lee, P. R.; Loebel, J. *Chem. Ber.* **1989**, *22*, 1897. $Lu(C_5Me_5)_2(C,N\text{-}\eta^2\text{-}C_5H_4N)$ has been structurally characterized, but the Lu–N distance was not reported: Watson, P. L. *J. Chem. Soc., Chem. Commun.* **1983**, 276. In $(C_5Me_5)_2Sm(bpy)$ the dative Sm–N distances are 2.427 and 2.436 Å: Evans, W. J.; Drummond, D. K. *J. Am. Chem. Soc.* **1989**, *111*, 3329. In the $\mu\text{-}N_2$ complex $(C_5Me_5)_2Sm(\mu\text{-}N_2)Sm(C_5Me_5)_2$, Sm–N is 2.347 Å: Evans, W. J.; Ulibarri, T. A.; Ziller, J. W. *J. Am. Chem. Soc.* **1988**, *110*, 6877. Ln–N distances in $(C_5H_5)_3Ln(py)$ (Ln = Sm, Nd) complexes are tabulated in: Deacon, G. B.; Gatehouse, B. M.; Platts, S. N.; Wilkinson, D. L. *Aust. J. Chem.* **1987**, *40*, 907. We note, however, that in electron-deficient $Ti(C_5Me_5)_2$ amides, no indication of $p_\pi\text{–}d_\pi$ donation from N to Ti was found: Feldman, J.; Calabrese, J. C. *J. Chem. Soc., Chem. Commun.* **1991**, 1042. It has also been suggested that linear imido ligands do not necessarily donate their lone pair to the metal: Kee, T. P.; Schofield, M. H.; Schrock, R. R. *J. Am. Chem. Soc.* **1990**, *112*, 1642.

(16) (a) Jeske, G.; Lauke, H.; Mauermann, H.; Swepston, P. N.; Schumann, H.; Marks, T. J. *J. Am. Chem. Soc.* **1985**, *107*, 8091. (b) Den Haan, K. H.; De Boer, J. L.; Teuben, J. H.; Spek, A. L.; Kojic-Prodic, B.; Hays, G. R.; Huis, R. *Organometallics* **1986**, *5*, 1726. (c) Heeres, H. J.; Renkema, J.; Booij, M.; Meetsma, A.; Teuben, J. H. *Organometallics* **1988**, *7*, 2495.

97 (5)°; the sum of the remaining Lu–C–Si and Si–C–Si angles = 345.9 (7)°].

Few porphyrin lanthanide, scandium, or yttrium (or actinide) complexes have been structurally characterized (Table V).

These complexes also display saucer-shaped porphyrins with the large metal ion displaced from the N_4 plane, the four nitrogen atoms forming the bottom of the dish with its convexity toward the metal atom. This distortion serves to optimize σ and π bonding between the nitrogen atoms and the metal, as it allows the sp^2 hybrid lone pair to point toward the metal rather than into the N_4 porphyrin plane. A complementary crystallographic and solution ^1H NMR study[17] of peripherally crowded zinc(II) porphyrins showed that, in this case at least, the conformational distortion is retained in solution.

Compound **1** serves as a versatile starting material for a range of new lutetium porphyrin species, the alkyl ligand being susceptible to controlled protonolysis under mild conditions (Scheme I). Thus, reaction of $(OEP)MCH(SiMe_3)_2$ with 2,6-di-*tert*-butylphenol (1 equiv) affords purple, crystalline $(OEP)MO\text{-}2,6\text{-}C_6H_3{}^tBu_2$ (M = Lu (**2a**), Y (**2b**)) quantitatively. Protonolysis of the OEP ligand is not observed.

$$(OEP)MCH(SiMe_3)_2 + HOC_6H_3{}^tBu_2 \rightarrow \underset{\mathbf{2}}{(OEP)MOC_6H_3{}^tBu_2} + CH_2(SiMe_3)_2$$

A direct, more convenient, and synthetically superior approach to complexes **2a** and **2b** is by heating $M(OC_6H_3{}^tBu_2)_3$ (M = Lu, Y) with $OEPH_2$ (1 equiv, 100 °C, 16 h, toluene) to give **2a** and **2b** in 88% and 63% isolated yield, respectively. See also Scheme I.

$$M(OC_6H_3{}^tBu_2)_3 + OEPH_2 \rightarrow \underset{\mathbf{2}}{(OEP)MOC_6H_3{}^tBu_2} + 2HOC_6H_3{}^tBu_2$$

An intermediate $(OEP)M(OC_6H_3{}^tBu_2)_2$ species, with only one porphyrin nitrogen σ-bonded to M, is not observed. The steric bulk of the attendant ligands in **2** and the steric hindrance of the liberated phenol effectively inhibits its coordination to **2**. Hexane-insoluble **2** is conveniently and easily separated from $HOC_6H_3{}^tBu_2$ by washing with hexane. The isotropic shift induced by the proximate porphyrin ring on an axial substituent is a useful diagnostic tool and is reflected in the phenoxide CMe_3 groups being shifted upfield to −0.67 ppm (Lu) or −0.64 ppm (Y).

Complexes **2a** and **2b** are potentially useful precursors to prepare alkyl derivatives of the (OEP)M fragment, since loss of $LiOC_6H_3{}^tBu_2$ circumvents problems[9] associated with salt coordination. Thus, reaction of $(OEP)MOC_6H_3{}^tBu_2$ [M = Lu (**2a**), Y (**2b**)] with $LiCH(SiMe_3)_2$ (1 equiv) cleanly affords **1a** and **1b**. This route is synthetically much more convenient and efficient than the alternative route via $M\{CH(SiMe_3)_2\}_3$, as it requires just 1 rather than the 3 equiv of $LiCH(SiMe_3)_2$ necessary to convert $M(OC_6H_3{}^tBu_2)_3$ to $M\{CH(SiMe_3)_2\}_3$.

$$\underset{\mathbf{2}}{(OEP)MOC_6H_3{}^tBu_2} + LiCH(SiMe_3)_2 \rightarrow \underset{\mathbf{1}}{(OEP)MCH(SiMe_3)_2} + LiOC_6H_3{}^tBu_2$$

In some recently published related Sc chemistry, metathesis of (OEP)ScCl with LiX in THF (X = $CH(SiMe_3)_2$, $N(SiMe_3)_2$, C_5H_5) has been shown to give $(OEP)ScX$[3b] (see also Table V). The smaller size of Sc^{3+}, in comparison with Lu^{3+} or Y^{3+}, ensures that LiCl or THF coordination does not play a significant role. Organolanthanide chemistry is not so readily amenable to such synthetic methodology, due to problems associated with salt and donor solvent coordination.

Reaction of $(OEP)LuCH(SiMe_3)_2$ with excess $^tBuC_2H$ (3 h, 25 °C) quantitatively yields the alkynyl complex $[(OEP)LuC_2{}^tBu]_2$ (**3a**). Reaction of isolated **3a** with excess $^tBuC_2H$ at 60 °C did not lead to its catalytic dimerization (Scheme II).

(17) Barkigia, K. M.; Berber, M. D.; Fajer, J.; Medforth, C. J.; Renner, M. W.; Smith, K. M. *J. Am. Chem. Soc.* **1990**, *112*, 8851.

Table VI. Representative[a] ^1H NMR Chemical Shifts (δ) of OH Groups

compd	O*H* ^1H NMR chem shift	ref
$(OEP)Y(\mu\text{-}OH)_2Y(OEP)$	−8.18	this work
$(OEP)Lu(\mu\text{-}OH)_2Lu(OEP)$	−7.18	this work
$[(OEP)Th(OH)_2]_3(OH_2)_2$	−4.36	19a
$[(TTP)Th(OH)_2]_3(OH_2)_2$	−3.88	19a
$[(C_5H_5)_2Y(\mu\text{-}OH)]_2\cdot PhC_2Ph$		19d
$[O(CH_2CH_2C_5H_4)_2Y]_2(\mu\text{-}N_2C_3HMe_2)(\mu\text{-}OH)$	9.15	19e
$(C_5Me_5)_2Zr(OH)_2$	3.47	18
$(C_5Me_5)_2Hf(OH)_2$	2.98	18
$(OEP)Ge(C_6H_5)(OH)$	−5.82	19b

[a] For brevity and comparison purposes late transition metal hydroxide complexes have been excluded.

Discrete mononuclear early transition metal hydroxide species[18] as well as the (di- or trimeric) organolanthanide/actinide hydroxides[4a,19a,d,e] are very rare, an ubiquitous decomposition pathway being bimolecular elimination of water to yield the thermodynamically more stable μ-oxo species.

$$2M\text{–}OH \rightarrow M\text{–}O\text{–}M + H_2O$$

Compounds **1** are cleanly hydrolyzed by H_2O (1 equiv) to give the hydroxides $[(OEP)MOH]_2$ [M = Lu (**4a**), Y (**4b**)], with concomitant formation of $CH_2(SiMe_3)_2$ (1 equiv) (Scheme II). As in **1** and **2** the porphyrin ethyl resonances of **3** and **4** are diastereotopic. In contrast to monomeric **1** and **2**, the porphyrin methyne protons of compounds **3** and **4** display a high-field shift[4c] to ca. 9.6 ppm. In contrast, in monomeric diamagnetic 1:1 octaethylporphyrin–metal complexes the methyne protons invariably resonate in the narrow range δ 10.0–10.7 ppm.[20] Thus, compounds **3** and **4** are dimeric with bridging acetylide[21] and hydroxide[2d] groups, respectively, the high-field methyne chemical shift being due to the mutual influence of two porphyrin ring currents in a dimer. The O*H* resonance of compounds **4a** and **4b** is a two hydrogen singlet at −7.18 ppm (Lu) and −8.18 ppm (Y). This unusually high-field chemical shift[19] of the hydroxide is due to strong shielding by the porphyrin ring currents in dimeric **4**, as alluded to in Table VI.

The Soret band of **4a** in anhydrous, anaerobic toluene is at 383.2 nm, with additional bands at 494, 537, and 573 nm. These are in good agreement with those previously reported[4a] for "(OEP)-LuOH". "(OEP)LuOH" was prepared using aqueous workup procedures, and thus contains coordinated water (vide infra), hence is probably better formulated as $[(OEP)LuOH\cdot xH_2O]_n$ (n = 1, 2). In addition, an unreported[4a] absorption at 334 nm is observed. The Soret band in **4a** is hypsochromically shifted in comparison with metal monoporphyrin species,[20b] strongly indicative[4c] of the dimeric nature of **4a**. A Soret band blue shift (of 6 nm) was observed[4a] for "(OEP)LuOH" on increasing its concentration from 0.65 to 65 μM, suggesting that in very dilute solution [(OEP)-

(18) Hillhouse, G. L.; Bercaw, J. E. *J. Am. Chem. Soc.* **1984**, *106*, 5472 and references therein.

(19) (a) $[(OEP)Th(OH)_2]_3(OH_2)_2$: Kadish, K. M.; Liu, Y. H.; Anderson, J. E.; Charpin, P.; Chevrier, G.; Lance, M.; Nierlich, M.; Vigner, D.; Dormond, A.; Belkalem, B.; Guilard, R. *J. Am. Chem. Soc.* **1988**, *110*, 6455. (b) (OEP)Ge(OH)Ph: Kadish, K. M.; Xu, Q. Y.; Barbe, J.-M.; Anderson, J. E.; Wang, E.; Guilard, R. *J. Am. Chem. Soc.* **1987**, *109*, 7705. (c) Bryndza, H. E.; Fong, L. K.; Paciello, R. A.; Tam, W.; Bercaw, J. E. *J. Am. Chem. Soc.* **1987**, *109*, 1444. (d) Evans, W. J.; Hozbor, M. A.; Bott, S. G.; Robinson, G. H.; Atwood, J. L. *Inorg. Chem.* **1988**, *27*, 1990. (e) Schumann, H.; Loebel, J.; Pickardt, J.; Qian, C.; Xie, Z. *Organometallics* **1991**, *10*, 215.

(20) (a) Scheer, M.; Katz, J. J. In *Porphyrins and Metalloporphyrins*; Smith, K. M., Ed.; Elsevier: Amsterdam, 1975; p 461. (b) *Ibid*, pp 864–866.

(21) (a) Atwood, J. L.; Hunter, W. E.; Wayda, A. L.; Evans, W. J. *Inorg. Chem.* **1981**, *20*, 4115. (b) Evans, W. J.; Bloom, I.; Hunter, W. E.; Atwood, J. L. *Organometallics* **1983**, *2*, 709. (c) Nolan, S. P.; Stern, D.; Marks, T. J. *J. Am. Chem. Soc.* **1989**, *111*, 7844.

(22) (a) Gerothanassis, I. P.; Momenteau, M.; Loock, B. *J. Am. Chem. Soc.* **1989**, *111*, 7006. (b) Gerothanassis, I. P.; Momenteau, M. *J. Am. Chem. Soc.* **1987**, *109*, 6944.

Table VII. Representative ^{17}O NMR Chemical Shifts

compd	δ, ppm	ref
(OEP)Lu(μ-OH)$_2$Lu(OEP) (**4a**)	96	this work
(OEP)Y(μ-OH)$_2$Y(OEP) (**4b**)	100	this work
(OEP)Y(μ-OMe)$_2$AlMe$_2$ (**7**)	14	this work
$(C_5Me_5)_2Zr(OH)_2$	175	18
$(C_5Me_5)_2Zr(OH)Cl$	231	18
$[(C_5Me_5)_2ZrH]_2(\mu\text{-}O)$	581	18
$(C_5H_5)(CO)_3W\text{–}O\text{–}ZrCl(C_5H_5)_2$	194	24a
$(C_5H_5)_2W(H)\text{–}O\text{–}ZrCl(C_5H_5)_2$	247	24b
(η^3-HB(3-Bu^{t}pz)$_3$)MgOOR	102–183, 323–427	25
Fe–O_2 hemoprotein models	ca. 1750, ca. 2510	22a

LuOH·$xH_2O]_n$ (n = 1, 2) may be largely dissociated.

^{17}O NMR spectroscopy has been extensively used in zeolite and polyoxometalate chemistry[23] and is a useful diagnostic tool for characterizing oxo and hydroxo species.

To confirm the dimeric nature of **4**, ^{17}O-enriched [(OEP)YOH]$_n$ (**4b**) (n = 1, 2) was prepared from **1b** and $H_2{}^{17}O$ (35% ^{17}O enriched) with the expectation that the ^{17}O NMR spectrum would display coupling to one or two ^{89}Y ($I = {}^1/_2$, 100% abundant) nuclei. The ^{17}O NMR spectrum of [(OEP)Y^{17}OH]$_n$ (**4b**) displayed a broad peak at unusually high field δ = 100 ppm. The chemical shift of this resonance is temperature invariant; however, its width at half-maximum height (fwhm) ranges from >6000 Hz at −40 °C and 1760 Hz at 25 °C to 1140 Hz at 60 °C, due to dissociation/association of (OEP)M(μ-OH)$_2$M(OEP). This exchange phenomena is also temperature dependent, as given by the strong temperature dependence of the ^{17}O line width. Although a similar temperature-dependent broadening of the ^{17}O line width was observed[22b] in an iron porphyrin dioxygen complex, this was ascribed to an increase in the correlation time for molecular tumbling at the end-on bound O_2 moiety, an explanation not possible for **4b**. Neither coupling of ^{89}Y to ^{17}O could be observed in **4b**, nor does **4b** display yttrium coupling to the hydroxide proton, due to rapid intermolecular H exchange. The ^{17}O NMR chemical shift and line width of ^{17}O-enriched (OEP)Lu(μ-OH)$_2$Lu(OEP) (**4a**) are very similar to that for **4b**, μ-^{17}OH in **4a** resonating at δ = 96 ppm (fwhm = 1280 Hz at 25 °C).

For comparison, the ^{17}O NMR chemical shifts of terminal hydroxy, μ-oxo, alkyl peroxo, and hemoprotein models are given in Table VII.

In the series of complexes $MoO_nX_y(ligand)_2$ (n = 1–3; X = Br, Cl; y = 0, 2)[23] the chemical shifts of the oxo ligands displayed a good linear correlation with increasing Mo–O force constants, as well as with decreasing Mo–O bond length. This relatively high-field ^{17}O NMR chemical shift of the bridging hydroxide in **4a** and **4b** is therefore indicative of a weak M–O (M = Lu, Y) bond with little π character.[23] Linearity in M–O–M systems is due to strong π overlap of the oxygen lone pairs with vacant metal orbitals or to minimize steric repulsion between metal centers. Deviations from linearity are an indication of reduced π bonding, with nearly tetrahedral angles being observed in extreme cases.[26] It is pertinent to note that the μ-oxo bridge in [(TPP)Sc]$_2$(μ-O) is highly bent (Sc–O–Sc = 109 (3)°).[3a] The π character of these M–O or M–N bonds may be reduced as a consequence of preferential π donation from the OEP nitrogens, thus restricting multiple bonding between yttrium and the proximate oxygen in **4**, according to available molecular orbital arguments.

There is no tendency for μ-oxo formation from compounds **4**, although [(TPP)Sc]$_2$(μ-O), prepared via apparent bimolecular elimination of water from the related putative intermediate (TTP)ScOH, has been reported.[3a]

Scheme V

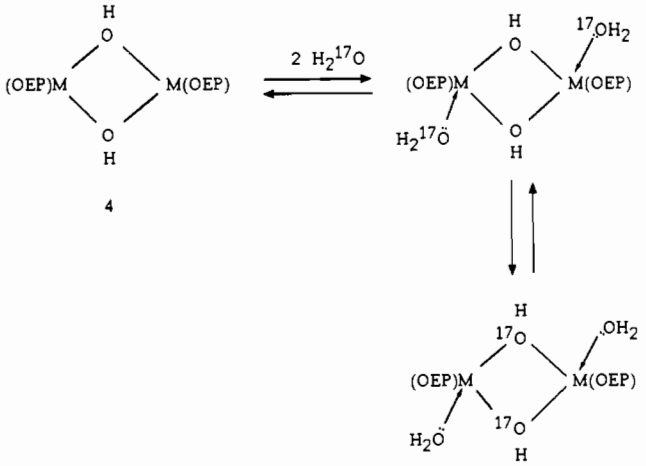

The monohydrates (OEP)MOH·H_2O (M = Lu, Y) can be prepared by addition of H_2O (2 equiv) to **1** or 1 equiv of H_2O to **4** in C_6D_6. These hydrates are most probably the octacoordinate dimers (OEP)M(μ-OH)$_2$(OH$_2$)$_2$M(OEP). Similar dimers of the type [(TTP)MOH·H_2O]$_2$ (M = Gd–Lu), containing bridging hydroxide and terminal water ligands, have been previously observed.[27] Decomposition of hydroxide species **4**, or their hydrates, by loss of $OEPH_2$ does not occur. They also display no tendency for μ-oxo formation.[3a] The reaction of (OEP)Lu(μ-OH)$_2$Lu(OEP) with H_2O in C_6D_6 was monitored by ^1H NMR spectroscopy. Addition of H_2O (1 equiv per Lu) yields (OEP)Lu(μ-OH)$_2$-(H$_2$O)$_2$Lu(OEP), which shows a broad six-proton ^1H NMR resonance at δ −2.2 ppm for the hydroxide and water protons. Progressive addition of H_2O (2 equiv per Lu) results in the ^1H NMR signal at δ −2.2 ppm increasing in intensity and steadily shifting downfield to δ −1.4 ppm. Its integrated intensity suggests that the hexahydrate [(OEP)Lu(μ-OH)$_2$Lu(OEP)]·$6H_2O$ is formed. At this juncture, no free H_2O is observed. Addition of more H_2O results in the appearance of free H_2O at ca. 5 ppm without an increase in the intensity of the resonance for coordinated water (now) at −1.0 ppm. In the limiting case with ca. 50 equiv of H_2O added, coordinated H_2O is at −0.4 ppm. The hydrates (OEP)Lu(μ-OH)$_2$Lu(OEP)·nH_2O are stable in the presence of excess water, and subsequent decomposition is not observed.

The question of oxygen exchange between the hydroxide **4** and coordinated water has been addressed by ^{17}O-labeling studies (Scheme V).

Addition of $H_2{}^{17}O$ (2 equiv) to [(OEP)Lu(μ-OH)]$_2$ (**4a**) in C_6D_6 under N_2 gave, after 30 min, a ^{17}O NMR spectrum showing peaks at 1.2 ppm and 13 ppm, attributable to free and coordinated $H_2{}^{17}O$, respectively. ^1H NMR monitoring of this reaction showed no resonance for free water (vide supra), suggesting that exchange of protons is faster than exchange between free and coordinated water. After ca. 3 h, a peak in the ^{17}O NMR spectrum at 30 ppm is observed, tentatively indicative of reversible ^{17}O exchange into the bridging hydroxide sites. Although **4a** has δ(^{17}O) = 96 ppm, the influence of coordinated water on the ^{17}O NMR chemical shift in **4a**·nH_2O is unclear.

The putative hydride [(OEP)MH]$_2$ (M = Lu, Y) could not be prepared, as (OEP)MCH(SiMe$_3$)$_2$ (M = Lu, Y) is resistant to hydrogenolysis. This is in marked contrast to the facile (1 bar, 0 °C, 30 min) σ-bond metathesis reaction of M(C$_5$Me$_5$)$_2$CH-(SiMe$_3$)$_2$ (M = La, Nd, Ce, Y)[16] with H_2. Reaction of (OEP)MCH(SiMe$_3$)$_2$ with H_2 (20 bar, 3 days, C_6D_{12}, 25 °C, in a stirred 25-mL autoclave equipped with a glass linear or high-pressure sapphire NMR tube[28]) led to the quantitative recovery

(23) (a) Miller, K. F.; Wentworth, R. A. D. *Inorg. Chem.* **1979**, *18*, 984. (b) Filowitz, M.; Ho, R. K. C.; Klemperer, W. G.; Shum, W. *Inorg. Chem.* **1979**, *18*, 93. (c) Klemperer, W. G. *Angew. Chem., Int. Ed. Engl.* **1978**, *17*, 246.

(24) (a) Jacobsen, E. N.; Trost, M. K.; Bergman, R. G. *J. Am. Chem. Soc.* **1986**, *108*, 8092. (b) Jacobsen, E. N. Ph.D. Thesis, University of California, Berkeley, CA, 1986.

(25) Han, R.; Parkin, G. *J. Am. Chem. Soc.* **1990**, *112*, 3662. Han, R.; Parkin, G. *Polyhedron* **1990**, *9*, 2665, ref 5.

(26) Jezovska-Trzebiatowska, B. *Coord. Chem. Rev.* **1968**, *3*, 255. San Filippo, J., Jr.; Grayson, R. L.; Srudoch, H. J. *Inorg. Chem.* **1976**, *15*, 269.

(27) Hammerschmitt, P. Ph.D. Thesis, Technische Hochschule, Darmstadt, Germany, 1987.

Scheme VI

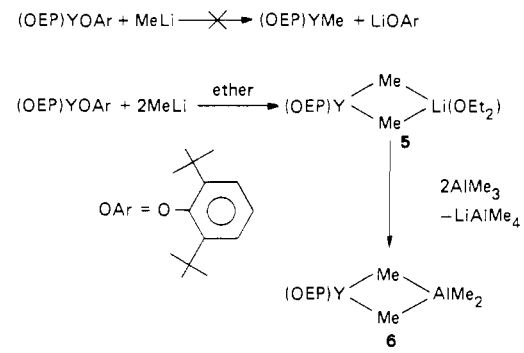

of $(OEP)MCH(SiMe_3)_2$, *without* trace of $CH_2(SiMe_3)_2$.

Although both $(OEP)MCH(SiMe_3)_2$ and $M(C_5Me_5)_2CH(SiMe_3)_2$ are formally 14-electron species (assuming maximum possible π donation from the porphyrin nitrogen atoms), they clearly possess very different electronic properties and coordination geometries arising from their coordination spheres. Research in late transition metal chemistry[29a] on bond dissociation enthalpies shows that, in general, a metal–hydride bond is ca. 20 kcal/mol stronger than the corresponding metal–alkyl bond.[1a] In d^0 transition metal and organolanthanide/actinide complexes this difference $D(Ln–H) - D(Ln–C)$ is reduced to ca. 5 kcal/mol due to the lack of d electrons, which would repel coordinated carbanions.[29b] From bond dissociation enthalpy data, hydrogenation of $Sm(C_5Me_5)_2CH(SiMe_3)_2$ has been calculated[30] to be thermoneutral. In addition, the absence of a cis coordination site, as required for a four-center σ-bond metathesis reaction, kinetically inhibits hydrogenation of these pyramidal five-coordinate porphyrin alkyl complexes. In contrast, protonolysis of **1** to afford **2**–**4** is facile, presumably via an induced dipole X–H bond heterolysis mechanism and favorable product thermodynamics (formation of strong M–O and metal–acetylide bonds). It is also pertinent regarding the kinetic and thermodynamic stability of **1** toward H_2 that the crystal structure of $(OEP)LuCH(SiMe_3)_2$ (**1a**) shows no distortion of the $CH(SiMe_3)_2$ group through interaction of a γ-Me group with the Lu atom. In contrast to the structure of $Ln(C_5Me_5)_2CH(SiMe_3)_2$,[16] there is no inherent tendency in **1a** (from crystallographic data) for (intramolecular) σ-bond coordination to Lu, despite the formally electron-deficient metal.

The "hard" donor properties and different coordination geometry imposed by the octaethylporphyrin ligand are responsible for this marked difference in reactivity, compared to $Ln(C_5Me_5)_2CH(SiMe_3)_2$.[16] In the series $(C_5Me_5)_2LnR$, $[Me_2Si(C_5Me_4)_2]LnR$, and $[Et_2Si(C_5Me_4)(C_5H_4)]LnR$ (R = $CH(SiMe_3)_2$) the decreasing Ln–R hydrogenolysis reactivity was ascribed[30a] to reduced charge stabilization at the lanthanide metal in the heterolytic, four-center hydrogenolysis transition state rather than to thermodynamic factors. Hard, electronegative ancillary ligands weaken Ln–H bonds compared to Ln–alkyl, due to the former's relative thermodynamic instability and to the additional electropositivity of the proximate lanthanide center (compared with its C_5Me_5 counterpart[30,31]), although the hydride may derive additional stabilization by bridging the electropositive center. The two β-silicons of $CH(SiMe_3)_2$ also delocalize the partial negative charge.

Scheme VII

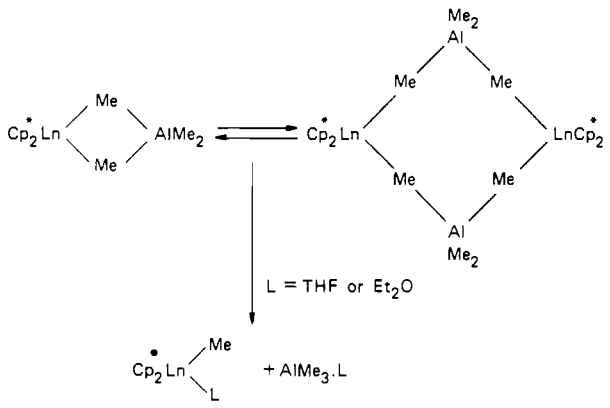

Scheme VIII

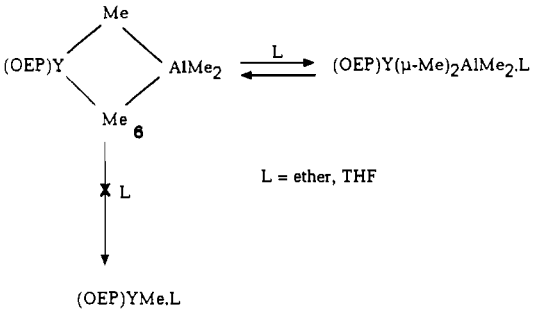

The influence of ancillary ligands on the propensity for olefin insertion and hydrogenolysis in f-element chemistry has been addressed thermochemically[30] as well as theoretically.[7] The additional electrophilicity at Lu and Y induced by the porphyrin ligand (compared to its $(C_5Me_5)_2$ counterparts[16]) should serve to strengthen M–R relative to M–H. π Donation, while undoubtedly possible, is a secondary effect compared with the electronegativity of nitrogen and may not be particularly significant[31] in comparing the influence of a porphyrin (or aryloxide) ligand with C_5Me_5.

Although putative $[(OEP)MH]_2$ proved to be inaccessible, we were interested in preparing $[(OEP)MMe]_n$ (n = 1, 2), having already ascertained that aryloxides **2** could be alkylated to afford **1**. Methyl species $M(C_5Me_5)_2Me$ (M = Sc,[32] Lu,[33] Y[33]) have an extensive reactivity including propylene oligomerization[33b] and methane transmetalation.[32,33c]

Reaction of $(OEP)YOC_6H_3{}^tBu_2$ (**2b**) with MeLi (2 equiv) in ether (−40 → 20 °C) afforded bright red, ether-insoluble $(OEP)Y(\mu\text{-}Me)_2Li(OEt_2)$ (**5**), with concomitant formation of inert $LiOC_6H_3{}^tBu_2{\cdot}OEt^2$ (Scheme VI).[10] Reaction of **2b** with just 1 equiv of MeLi leads to a 1:1 mixture of **2b** and **5**, demonstrating the strong tendency to form "ate" complexes, if sterically accessible. Although the heavier alkali metals are less likely to form such adducts, reaction of **2b** with solid KMe in hexane did not yield a tractable species. Coordinated MeLi can be readily removed by reaction of a suspension of **5** in hexane with $AlMe_3$ (2 equiv) to afford toluene- and hexane-soluble, deep red, monomeric $(OEP)Y(\mu\text{-}Me)_2AlMe_2$ (**6**) in excellent yield, which is readily

(28) Roe, C. *J. Magn. Reson.* **1985**, *63*, 388.
(29) (a) Halpern, J. *Inorg. Chim. Acta* **1985**, *100*, 41. (b) Ziegler, T.; Tschinke, V.; Versluis, L.; Baerends, E. J.; Ravenek, W. *Polyhedron* **1988**, *7*, 1625.
(30) (a) Nolan, S. P.; Stern, D.; Hedden, D.; Marks, T. J. In *Bonding Energetics in Organometallic Compounds*; Marks, T. J., Ed.; ACS Symposium Series 428; American Chemical Society: Washington, DC, 1990; p 159. (b) Bruno, J. W.; Stecher, H. A.; Morss, L. R.; Sonnenberger, D. C.; Marks, T. J. *J. Am. Chem. Soc.* **1986**, *108*, 7275. (c) Nolan, S. P.; Stern, D.; Marks, T. J. *J. Am. Chem. Soc.* **1989**, *111*, 7844. (d) Sonnenberger, D. C.; Morss, L. R.; Marks, T. J. *Organometallics* **1985**, *4*, 352. (e) Lin, Z.; Marks, T. J. M. *J. Am. Chem. Soc.* **1987**, *109*, 7979. Other effects are electronegativity and orbital repulsion. The electron affinities of the cyclopentadienyl radical and Cl are similar, so a Ln–(C_5Me_5) bond may be very polar: Labinger, J. A.; Bercaw, J. R. *Organometallics* **1988**, *7*, 926.
(31) The ^{89}Y NMR spectra (in C_6D_6) of a series of related yttrium complexes have been measured and led to C_5Me_5, $OC_6H_3{}^tBu_2$, and $CH(SiMe_3)_2$ group contributions to the ^{89}Y NMR chemical shift. Schaverien, C. J.; Frijns, J. H. G.; Heeres, H. J.; van den Hende, J. R.; Spek, A. L.; Teuben, J. H. *J. Chem. Soc., Chem. Commun.* **1991**, 642.
(32) Thompson, M. E.; Baxter, S. M.; Bulls, A. R.; Burger, B. J.; Nolan, M. C.; Santarsiero, B. D.; Schaefer, W. P.; Bercaw, J. E. *J. Am. Chem. Soc.* **1987**, *109*, 203.
(33) (a) Watson, P. L.; Parshall, G. W. *Acc. Chem. Res.* **1985**, *18*, 51. (b) Watson, P. L. *J. Am. Chem. Soc.* **1982**, *104*, 337. (c) Watson, P. L. *J. Am. Chem. Soc.* **1983**, *105*, 6491. (d) Watson, P. L.; Roe, D. C. *J. Am. Chem. Soc.* **1982**, *104*, 6471.

Scheme IX

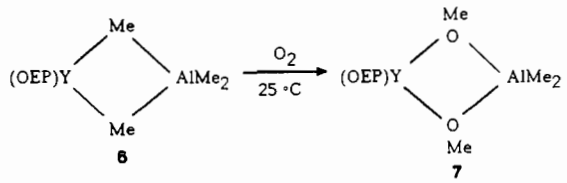

separated from insoluble $LiAlMe_4$. Reaction of **5** with just 1 equiv of $AlMe_3$ does not lead to (OEP)YMe and $LiAlMe_4$ but to a 1:1 mixture of **5** and **6**. The ethyl protons of the OEP ligand in **6** are also diastereotopic and give rise to an ABX_3 spin system with J_{AB} = 17 Hz and $J_{AX} = J_{BX}$ = 7.6 Hz (simulated spectra). Even at −60 °C only one peak for all aluminum methyl groups is observed at −8.96 ppm [$^1J_{CH}$ = 109 Hz], while the octaethylporphyrin resonances remained sharp, indicating a highly fluxional coordination of the $AlMe_4$ moiety. This lack of yttrium coupling or separate methyl resonances for the $Y(\mu\text{-}Me)_2AlMe_2$ unit in the low-temperature ^{13}C NMR spectrum is in contrast to the related cyclopentadienyl analogues $(C_5R_5)_2Y(\mu\text{-}Me)_2AlMe_2$ (R = H, Me).[34,35a]

In contrast to the observed reactivity of $(C_5R_5)_2Ln(\mu\text{-}Me)_2AlMe_2$[34,35b] (Scheme VII), splitting of the $Y(\mu\text{-}Me)_2AlMe_2$ bridge in **6** with THF or ether gives only reversible adduct formation (Scheme VIII). Addition of C_5H_5N or 4-(dimethylamino)pyridine[36] (1 equiv) led to decomposition. We are currently investigating other synthetic strategies to effect this transformation. The characterization, physical properties, and comparison of the reactivity of **6** with its C_5H_5 and C_5Me_5 counterparts has already been reported.[8] In particular, there is no temperature-dependent monomer–dimer equilibrium as has been observed[34] for the more sterically hindered C_5Me_5 analogues of **6**.

Biomimetic approaches toward mimicking the chemistry of monooxygenase enzymes, particularly cytochrome P450, have focused on the metalloporphyrin moiety and its interaction with oxygen donors, solvents, and substrates.[1b,37] Studies of metal–dioxygen systems and the reaction of dioxygen with metal complexes have concentrated on varying the central metal atom using late transition metals that closely resemble the characteristics of the iron–heme found in cytochrome P450.[37] Insertion of O_2 into metal–alkyl bonds has also been studied.[25a,38,39] Wolczanski has studied the activation of dioxygen using (tritox)M (tritox = OC^tBu_3; M = Ti, Zr, Hf) systems to afford dimethoxy complexes, presumably via an $M(\eta^2\text{-}OOMe)Me$ intermediate.[38] Reaction of O_2 with In^tBu_3 and $\{\eta^3\text{-}HB(3\text{-}Bu^tpz)_3\}MgR$ gives the isolable alkyl peroxy species $[^tBu_2In(\mu\text{-}OO^tBu)]_2$[39] and $\{\eta^3\text{-}HB(3\text{-}Bu^tpz)_3\}MgOOR$,[25] respectively. Their stability was attributed to their sterically demanding ligand environment inhibiting bimolecular oxygen atom abstraction. $(OEP)GeR_2$ reacts with O_2 photochemically to give (OEP)GeR(OOR) and $(OEP)Ge(OOR)_2$.[40] We were intrigued by the possibility that the inherent oxophilicity associated with early transition metal or lanthanide porphyrin complexes,[41] and the robustness of the (OEP)Ln unit, might facilitate stabilization of new intermediates. Selective activation of O_2 by lanthanide complexes has not been previously observed, despite their intrinsic oxophilicity and frequently observed decomposition by exposure to oxygen.

Scheme X

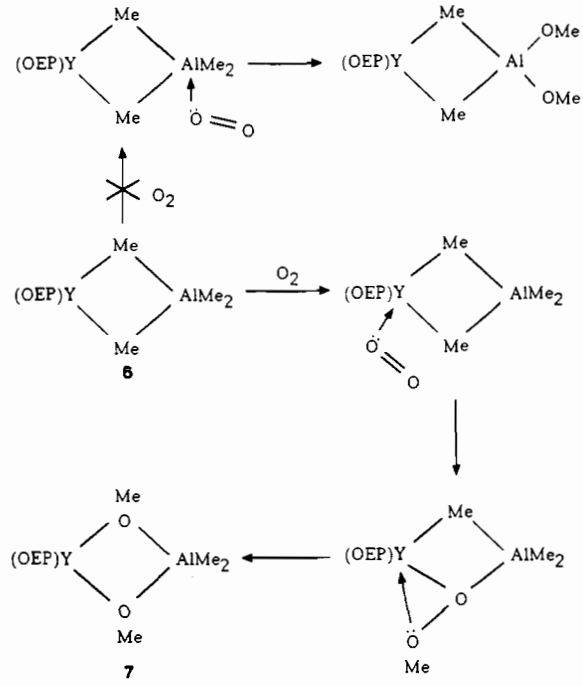

$(OEP)Y(\mu\text{-}Me)_2AlMe_2$ (**6**) activates O_2 at room temperature to afford $(OEP)Y(\mu\text{-}OMe)_2AlMe_2$ (**7**) selectively. Addition of excess dry O_2 to a hexane solution of **6** results in its rapid and quantitative conversion to **7**. ^1H NMR monitoring of the reaction carried out in C_6D_6 shows **7** to be the only species formed. This reaction can also be performed simply by aerial oxidation. There is no further oxidation of **7** to, for example, $(OEP)Y(\mu\text{-}OMe)_2Al(OMe)_2$ (Scheme IX).

In contrast to the fluxional $Y(\mu\text{-}Me)_2AlMe_2$ unit in **6**, the $Y(\mu\text{-}OMe)_2AlMe_2$ fragment in **7** is static (at 25 °C). The bridging methoxy groups resonate at δ 0.76 ppm (^1H NMR) and at δ 46.9 ppm in the ^{13}C NMR spectrum. The terminal methyl groups resonate at −2.23 ppm (^1H NMR) and −14.1 ppm (fwhm = 35 Hz) (^{13}C NMR), these being typical ^1H and ^{13}C NMR chemical shifts for terminal Al–Me groups. The magnitude of the shielding due to the porphyrin ring current is most noticeable in the upfield ^1H NMR chemical shifts of the methoxy group.

To accumulate evidence pertinent to the mechanism of oxygen activation, **6** was treated with $^{17}O_2$ to allow investigation by ^{17}O NMR spectroscopy. Addition of excess (9 equiv) $^{17}O_2$ to a C_6D_6 solution of **6** (25 °C, 15 min) resulted in formation of ^{17}O-enriched **7**, which displays just one ^{17}O NMR resonance at 13.8 ppm (fwhm = 850 Hz).

The ^{17}O NMR chemical shifts of these (OEP)Y complexes resonate at high field in comparison with other metal–oxygen bound moieties for which ^{17}O NMR data are available. In the case of **7**, the ^{17}O NMR chemical shift is most reminiscent of simple organic ethers and methoxy compounds.[42] As expected, stirring ^{17}O-enriched **7** under an atmosphere of $^{16}O_2$ does not lead to exchange of the incorporated oxygen label. Furthermore, there is no subsequent reaction of **7** with excess dry O_2.

An alkyl peroxy species is a probable intermediate in the activation of dioxygen; therefore, it was of interest to prepare (OEP)YOOR (cf. $(OEP)Ge(OOR)_2$[40] above). Although $(OEP)YCH(SiMe_3)_2$ (**1**) undergoes clean protonolysis (vide su-

(34) (a) Busch, M. A.; Harlow, R.; Watson, P. L. *Inorg. Chim. Acta* **1987**, *140*, 15. (b) Evans, W. J.; Chamberlain, L. R.; Ulibarri, T. A.; Ziller, J. W. *J. Am. Chem. Soc.* **1988**, *110*, 6423. (c) Den Haan, K. H.; Wielstra, Y.; Eshuis, J. J. W.; Teuben, J. H. *J. Organomet. Chem.* **1987**, *323*, 181.
(35) (a) Holton, J.; Lappert, M. F.; Ballard, D. G. H.; Pearce, R.; Atwood, J. L.; Hunter, W. E. *J. Chem. Soc., Dalton Trans.* **1979**, 45. (b) Holton, J.; Lappert, M. F.; Ballard, D. G. H.; Pearce, R.; Atwood, J. L.; Hunter, W. E. *J. Chem. Soc., Dalton Trans.* **1979**, 54.
(36) Ott, K. C.; Grubbs, R. H. *J. Am. Chem. Soc.* **1981**, *103*, 5922. Lee, J. B.; Ott, K. C.; Grubbs, R. H. *J. Am. Chem. Soc.* **1982**, *104*, 7491.
(37) Sheldon, R. A.; Kochi, J. K. *Metal Catalyzed Oxidations of Organic Compounds*; Academic Press: New York, 1981. Mimoun, H. In *Comprehensive Coordination Chemistry*; Wilkinson, G., Gillard, R. D., McCleverty, J. A., Eds.; Pergamon: Oxford, England, 1988; Vol. 6, Chapter 1.
(38) Lubben, T. V.; Wolczanski, P. T. *J. Am. Chem. Soc.* **1987**, *109*, 424.
(39) Cleaver, W. M.; Barron, A. R. *J. Am. Chem. Soc.* **1989**, *111*, 8966.
(40) Cloutour, C.; Lafargue, D.; Pommier, J. C. *J. Organomet. Chem.* **1978**, *161*, 327.
(41) (a) Guilard, R.; Lecomte, C. *Coord. Chem. Rev.* **1985**, *65*, 87. (b) Holm, R. H. *Chem. Rev.* **1987**, *87*, 1401.
(42) Rodger, C.; Sheppard, N.; McFarlane, C.; McFarlane, W. In *NMR and the Periodic Table*; Harris, R. K., Mann, B. E., Eds.; Academic Press: London, 1978; pp 383.

pra), reaction with anhydrous[43] ^{t}BuOOH failed to yield an identifiable product. Neither did reaction of **1** with O_2.

Oxidation of simple aluminum alkyls with O_2 is very fast, and only the free-radical chain oxidation of the last, less reactive Al–C bond in R–Al(OR)$_2$ has been studied.[44,45] A considerable body of evidence has been accumulated to suggest that their oxidation proceeds via a free-radical chain mechanism.[46] A potential mechanism to explain the selective conversion of **6** to **7** involves initial attack at the more oxophilic, sterically less hindered yttrium center rather than at 4-coordinate aluminum, to form a bridging Y(η^2-OOMe)Al species. Insertion of the remaining Y(μ-Me)Al methyl group affords **7** (Scheme X).

Attack at Y, and its subsequent reduction in oxophilicity in **7** relative to **6**, explains why **7** is not further oxidized to e.g. (OEP)Y(μ-OMe)$_2$Al(OMe)$_2$. This suggests that Al, in both compounds **6** and **7**, is relatively inert, in comparison with Y, toward O_2 coordination. This is presumably a consequence of the relatively open yttrium environment together with attack at the 4-coordinate aluminum center being suppressed, relative to the situation in AlR_3.

Conclusions

The octaethylporphyrin ligand has been shown to be a robust and viable alternative to the bis(pentamethylcyclopentadienyl) ligand system in its ability to stabilize lanthanide alkyl complexes. In some cases, the chemistry of these (OEP)Ln complexes is more similar to their less sterically hindered, less electron-rich C_5H_5 counterparts[35,47] than their C_5Me_5 analogues.[34] The (OEP)Y moiety is sufficiently robust to allow the selective room-temperature activation of O_2. Despite the facile nature of the Al–Me → Al–OMe oxidation, it is noteworthy that oxidation of **6** yields **7** selectively, there being no further oxidation to (OEP)Y(μ-OMe)$_2$Al(OMe)$_2$. Coordination to (OEP)Y evidently effectively mediates the oxidation of the Al–Me bonds in **6**.

Experimental Section

All experiments were performed with the rigorous exclusion of water and oxygen in an argon atmosphere using Schlenk type glassware or in a Braun single-station drybox equipped with a −40 °C refrigerator under a nitrogen atmosphere. Elemental analyses were performed at Analytische Laboratorien, Elbach, West Germany. Nuclear magnetic resonance spectra were recorded on Varian XL-200 or Varian VXR-300 spectrometers. Chemical shifts are reported in parts per million and referenced to the residual protons in deuterated solvents. Coupling constants are reported in hertz. Coupling constants (J_{C-H}) were obtained from gated (^{1}H NOE enhanced) spectra. UV/vis spectra were recorded on a Perkin-Elmer Lambda 9 spectrometer between 300 and 800 nm. Anhydrous $LuCl_3$ was purchased from Micropure, Driebergen-Rijsenb., The Netherlands. Octaethylporphyrin was prepared by literature procedures.[48] Anhydrous ^{t}BuOOH was purchased from Aldrich and used as received. $H_2{}^{17}O$ (35% enriched) was purchased from ICON. $^{17}O_2$ (22% enriched) was purchased from Isotec. Deuterated solvents were dried over 4-Å molecular sieves. Solvents were P. A. grade. Ether, hexane, and toluene were dried initially over sodium wire and THF was dried over solid KOH, and then the solvents were distilled from the appropriate drying reagent (sodium benzophenone ketyl for ether and THF, sodium for hexane and toluene) under argon prior to use. M(O-2,6-C$_6$H$_3{}^t$Bu$_2$)$_3$ (M = Lu, Y) were prepared as described,[49] and M{CH(SiMe$_3$)$_2$}$_3$ (M = Lu, Y)[10a] by analogy (see below) to Ln{CH(SiMe$_3$)$_2$}$_3$ (Ln = La, Sm).[10b]

^{17}O NMR Measurements. ^{17}O NMR spectra were obtained on the Varian VXR-300 instrument operating at 40.662 MHz for ^{17}O. Spectra were run in C_6D_6 at 22 °C in a 10-mm NMR tube containing a microcell insert of volume ca. 0.8 mL, unless otherwise stated. Chemical shifts were referenced externally to a capillary containing $H_2{}^{17}O$, which was itself inserted in a 5-mm NMR tube containing C_6D_6 as deuterium lock. The setup of the spectrometer was checked using 70% v/v 1,4-dioxane in C_6D_6. Under these accumulation conditions this gave a peak at −1.2 ppm (fwhm = 110 Hz) at 22 °C. The pulse width was 19.3 μs. The signal to noise was improved by applying a 30-Hz exponential broadening factor to the FID prior to Fourier transformation. A total of 500–1500 transients were typically accumulated.

Lu{CH(SiMe$_3$)$_2$}$_3$. A 1.34-g, 8.07-mmol, amount of LiCH(SiMe$_3$)$_2$ was added slowly as a solid to a colorless solution of 2.1 g, 2.66 mmol, of Lu(OC$_6$H$_3{}^t$Bu$_2$)$_3$[49] in 100-mL of hexane at 25 °C. A white suspension rapidly formed, which was stirred for 30 min at 25 °C and then filtered to remove LiOC$_6$H$_3{}^t$Bu$_2$. The volume of the colorless filtrate was reduced, and crystallization at −40 °C afforded Lu{CH(SiMe$_3$)$_2$}$_3$ as white fluffy needles. Yield: 0.92 g, 53%. ^{1}H NMR (C_6D_6): δ 0.308 (Si*Me*$_3$), −0.82 (C*H*). ^{13}C NMR (C_7D_8, 25 °C): δ 57.35 (d, 90 Hz, *C*H), 3.69 (q, 116 Hz, Si*Me*$_3$). Anal. Calcd for Lu{CH(SiMe$_3$)$_2$}$_3$·0.5hexane ($C_{24}H_{64}LuSi_6$): C, 41.40; H, 9.27; Lu, 25.13. Found: C, 41.2; H, 9.2; Lu, 24.57.

Y{CH(SiMe$_3$)$_2$}$_3$. To 1.36 g, 1.93 mmol, of Y(OC$_6$H$_3{}^t$Bu$_2$)$_3$ in 30 mL of hexane was added 0.96 g, 5.80 mmol, of LiCH(SiMe$_3$)$_2$ as a solid at 25 °C. A white suspension rapidly formed, which was stirred for 3 h at 25 °C and subsequently filtered to remove LiOC$_6$H$_3{}^t$Bu$_2$. The filtrate was reduced in volume and crystallized at −40 °C to afford 0.82 g (75% yield, two crops) of Y{CH(SiMe$_3$)$_2$}$_3$ as white needles. ^{1}H NMR (C_6D_6): δ 0.30 (s, 54 H), −0.59 (d, J_{YH} = 2.4 Hz, 3 H).

(OEP)LuCH(SiMe$_3$)$_2$ (1a). A 0.514-g, 0.788-mmol, amount of Lu{CH(SiMe$_3$)$_2$}$_3$ and 0.421 g, 0.786 mmol, of OEPH$_2$ were combined in a small bomb in 10 mL of benzene and heated in an oil bath at 60 °C for 6 h with stirring. The resulting purple homogeneous solution was allowed to cool to room temperature and the solvent removed under vacuum to give a red powder. (^{1}H NMR monitoring of the reaction showed the formation of only one product with no observable intermediates.) This was crystallized from hexane at −40 °C to give **1a**. ^{1}H NMR (C_6D_6, 25 °C): δ 10.62 (s, 4 H), 4.04 (m, ABX$_3$ system, 7.5, 14 Hz, C*H*$_2$), 1.94 ("t", ABX$_3$ system, 7.5 Hz, CH$_3$), −1.76 (s, 18 H, Si*Me*$_3$), −5.78 (s, 1 H, C*H*(SiMe$_3$)$_2$). ^{13}C NMR (C_6D_6, 25 °C): δ 147.39 and 143.36 (s, pyrrole quaternaries), 100.85 (d, J = 149 Hz, CH), 41.05 [d, J = 95 Hz, *C*H(SiMe$_3$)$_2$], 20.28 (t, J = 127 Hz, CH$_2$), 18.81 (q, J = 127 Hz, CH$_3$), 2.76 (q, J = 119 Hz, Si*Me*$_3$). Anal. Calcd for $C_{43}H_{63}LuN_4Si_2$: C, 59.6; H, 7.32; N, 6.48; Lu, 20.22. Found: C, 57.9; H, 7.00; N, 6.80; Lu, 20.96.

(OEP)Lu{CH(SiMe$_3$)$_2$}(μ-Cl)K (1a·KCl). To 0.180 g, 0.246 mmol, of Lu{CH(SiMe$_3$)$_2$}$_3$(μ-Cl)K[12] was added 0.200 g, 0.374 mmol, 1.5 equiv, of OEPH$_2$ in 4 mL of C_6D_6 in a small glass bomb, and the purple solution was heated for 4.5 h at 65 °C. The solution was cooled to room temperature and the solvent removed in vacuo. The resulting purple solid was washed with hexane and the solvent removed to give purple **1a**. The purple hexane-insoluble residue was then extracted with toluene to yield purple **1a**·KCl, which was recrystallized from hexane to give 0.050 g as purple crystals. The purple toluene insolubles were identified as OEPH$_2$ (0.040 g), which was recovered unchanged from the reaction. ^{1}H NMR (C_6D_6): δ 9.19 (CH), 4.37 and 3.94 (m, 16 H, diastereotopic CH$_2$'s), 1.65 ("t", 24 H, CH$_3$), −0.66 (SiMe$_3$), −1.95 [C*H*(SiMe$_3$)$_2$]. ^{13}C NMR (C_6D_6/CD_2Cl_2): δ 150.6 and 139.7 (s, pyrrole quaternary), 98.5 (d, J = 152 Hz, *C*H), 51.5 (d, J = 91 Hz, *C*H(SiMe$_3$)$_2$), 20.6 (t, J = 127 Hz, *C*H$_2$), 18.9 (q, J = 127 Hz, *C*H$_3$), 5.4 (q, J = 119 Hz, Si*Me*$_3$). Anal. Calcd for (OEP)LuCH(SiMe$_3$)$_2$·KCl (**1a**·KCl) ($C_{43}H_{63}ClLuN_4KSi_2$): C, 54.84; H, 6.74; N, 5.95; Cl, 3.76; Lu, 18.58; K, 4.15. Found: C, 54.82; H, 6.62; N, 6.07; Cl, 3.63; Lu, 18.42; K, 3.98.

(OEP)YCH(SiMe$_3$)$_2$ (1b). A 0.150-g, 0.262-mmol, amount of Y{CH(SiMe$_3$)$_2$}$_3$ and 0.140 g, 0.26 mmol, of OEPH$_2$ were combined in a small bomb in 5 mL of benzene and heated in an oil bath at 60 °C for 6 h with rapid stirring. The resulting purple homogeneous solution was

(43) "Anhydrous" ^{t}BuOOH may contain traces of water. Trace amounts of water have caused difficulties in Ti-catalyzed epoxidations. Hanson, R. M.; Sharpless, K. B. *J. Org. Chem.* **1986**, *51*, 1922.

(44) Davies, A. G.; Roberts, B. P. *J. Chem. Soc. B* **1968**, 1074. Eisch, J. J. In *Comprehensive Organometallic Chemistry*; Wilkinson, G., Stone, F. G. A., Abel, E. W., Eds.; Pergamon Press: London, 1982; Vol. 1, Chapter 6.

(45) Davies, A. G.; Roberts, B. P. *Acc. Chem. Res.* **1972**, *5*, 387.

(46) The commonly accepted mechanism[44,45] for the oxidation of simple aluminum alkyls is as follows:

$$AlR_3 + O_2 \rightarrow R_2AlOO^\bullet + R^\bullet$$

$$R^\bullet + O_2 \rightarrow ROO^\bullet$$

$$AlR_3 + ROO^\bullet \rightarrow R_2AlOOR + R^\bullet$$

$$R_2AlOOR + AlR_3 \rightarrow 2RAl(OR)_2$$

$$RAl(OR)_2 + O_2 \rightarrow ROOAl(OR)_2$$

$$ROOAl(OR)_2 + RAl(OR)_2 \rightarrow Al(OR)_3$$

(47) (a) Ballard, D. G. H.; Courtis, A.; Holton, J.; McMeeking, J.; Pearce, R. *J. Chem. Soc., Chem. Commun.* **1978**, 994. (b) Ballard, D. G. H.; Pearce, R. *J. Chem. Soc., Chem. Commun.* **1975**, 621.

(48) Whitlock, H. W.; Hanauer, R. *J. Org. Chem.* **1968**, *33*, 2169. *Porphyrins and Metalloporphyrins*; Smith, K. M., Ed.; pp 766.

(49) Hitchcock, P. B.; Lappert, M. F.; Singh, A. *J. Chem. Soc., Chem. Commun.* **1983**, 1499. Hitchcock, P. B.; Lappert, M. F.; Smith, R. G. *Inorg. Chim. Acta* **1987**, *139*, 183.

(50) *International Tables for X-ray Crystallography*; Kynoch Press: Birmingham, England, 1974; Vol. IV.

allowed to cool to room temperature and the solvent removed under vacuum to give (OEP)YCH($SiMe_3$)$_2$ as a red powder. Crystallization from hexane at −40 °C gave analytically pure **1b**. ^{1}H NMR (C_6D_6, 25 °C): δ 10.61 (s, 4 H), 4.03 (m, ABX_3 system, 7.5, 14 Hz, CH_2), 1.92 ("t", ABX_3 system, 7.5 Hz, CH_3), −1.73 (s, 18 H, $SiMe_3$), −5.33 (d, 1 H, ^2J(YH) = 2.5 Hz, C*H*($SiMe_3$)$_2$). Anal. Calcd for $C_{43}H_{63}YN_4Si_2$: C, 66.12; H, 8.13; Y, 11.38. Found: C, 65.98; H, 8.13; Y, 11.55.

(OEP)LuO-2,6-$C_6H_3{}^tBu_2$ (2a). A 0.790-g, 1.0-mmol, amount of Lu(O-2,6-$C_6H_3{}^tBu_2$)$_3$ and 0.535 g, 1.0 mmol, of $OEPH_2$ were added to a large (100 mL) glass bomb in 12 mL of toluene. After being heated in an oil bath at 100 °C for 16 h, the homogeneous, intense purple solution was allowed to cool to room temperature. The toluene was removed in vacuum and the residual red powder washed with 4 × 10 mL of hexane to remove 2,6-di-*tert*-butylphenol to afford 0.767 g of **2a** as a bright red powder. An additional 0.037 g can be obtained by evaporating the hexane washings to dryness and washing this with 3 × 5 mL of hexane. Total yield: 0.804 g, 88%. ^{1}H NMR (C_6D_6): δ 10.58 (s, 4 H), 6.27 (d, 2 H), 6.05 (t, 1 H), 4.02 (q, CH_2), 1.90 (t, CH_3), −0.67 (s, 18 H, ^{t}Bu). ^{13}C NMR (C_6D_6): δ 160.45 (s, C_{ipso}), 147.77 (s, pyrrole *C*), 143.51 (s, pyrrole *C*), 135.94 (s, C_o), 123.72 (d, C_m), 115.67 (d, C_p), 101.10 (d, meso *C*H), 32.62 (s, *C*Me_3), 28.09 (q, C*Me*$_3$), 20.48 (t, *C*H_2), 19.00 (q, *C*H_3). Anal. Calcd for $C_{50}H_{65}LuN_4O$: C, 65.77; H, 7.18; N, 6.14; Lu, 19.16. Found: C, 65.78; H, 6.88; N, 6.11; Lu, 19.40.

(OEP)YO-2,6-$C_6H_3{}^tBu_2$ (2b). A 1.00-g, 1.42-mmol, sample of Y(O-2,6-$C_6H_3{}^tBu_2$)$_3$ and 0.76 g, 1.42 mmol, of $OEPH_2$ were added to a large (100 mL) glass bomb in 50 mL of toluene. After being heated in an oil bath at 90 °C for 16 h, the homogeneous, intense purple solution was allowed to cool to room temperature. The toluene was removed in vacuum and the red powder washed with 4 × 5 mL of hexane to remove 2,6-di-*tert*-butylphenol. **2b** (0.74 g) was isolated as a bright red powder. Yield: 63%. ^{1}H NMR (C_6D_6): δ 10.54 (s, 4 H), 6.28 (d, 2 H), 6.05 (t, 1 H), 4.01 (q, CH_2), 1.85 (t, CH_3), −0.64 (s, 18 H, ^{t}Bu). Anal. Calcd for $C_{50}H_{65}YN_4O$: C, 72.62; H, 7.92; Y, 10.75. Found: C, 72.77; H, 7.88; Y, 10.85.

[(OEP)LuC$_2{}^t$Bu]$_2$ (3a). A 0.10-g sample of (OEP)LuCH($SiMe_3$)$_2$ was dissolved in 15 mL of toluene in a small bomb and 60 μL of *tert*-butylacetylene added. The solution was allowed to stand for 15 h at 25 °C and the toluene removed in vacuo. The resulting residue was washed with 2 × 1 mL of hexane to afford [(OEP)LuC$_2{}^t$Bu]$_2$ as a purple crystalline solid. ^{1}H NMR (CD_2Cl_2): δ 9.77 (s, 4 H, CH), 4.08 (m, *J* = 7.5, 14 Hz, CH_2), 1.68 ("t", *J* = 7.5 Hz, CH_3), −1.00 (s, 9 H, ^{t}Bu). ^{1}H (C_6D_6): δ 9.96 (s, 4 H, CH), 4.10 (m, *J* = 7.5, 14 Hz, CH_2), 1.74 ("t", *J* = 7.5 Hz, CH_3), −0.66 (s, 9 H, ^{t}Bu). Anal. Calcd for $C_{84}H_{106}Lu_2N_8$: C, 63.95; H, 6.77; Lu, 22.18. Found: C, 63.70; H, 6.77; Lu, 22.45.

(OEP)Lu(μ-OH)$_2$Lu(OEP) (4a). Due to the synthetic difficulties associated with accurately adding exactly 1 equiv of H_2O (2.1 μL on a 100-mg scale) and the ensuing formation of hydrates (vide infra) with excess water, the hydrolysis is best achieved by exposing (OEP)LuCH($SiMe_3$)$_2$ as a finely powdered crystalline solid to atmospheric moisture for 15 min. In a solid-state reaction, 0.07 g of powdered (OEP)LuCH($SiMe_3$)$_2$ (**1a**) in a small vial was removed from the drybox and exposed to laboratory air for 10 min. (Exposure to atmospheric moisture for longer periods affords (OEP)Lu(μ-OH)$_2$(H_2O)$_2$Lu(OEP).) The vial was then returned to the drybox and the red-purple powder washed with 2 × 0.5 mL hexane to afford (OEP)Lu(μ-OH)$_2$Lu(OEP). ^{1}H NMR (C_6D_6): δ 9.64 (s, 8 H, CH), 3.83 and 3.76 (m, 32 H, AB, CH_2), 1.65 (m, 48 H, CH_3), −7.18 (s, 2 H, Lu–OH). ^{17}O NMR (C_6D_6, 25 °C): δ 96.2 ppm, fwhm = 1280 Hz. Anal. Calcd for $C_{72}H_{90}Lu_2N_8O_2$: C, 59.66; H, 6.26. Found: C, 59.54; H, 6.32.

(OEP)Lu(μ-OH)$_2$(H_2O)$_2$Lu(OEP). In the drybox, a weighed amount of (OEP)Lu(μ-OH)$_2$Lu(OEP) was dissolved in C_6D_6 in a 5-mm NMR tube equipped with a septum cap. The tube was removed from the box, and known amounts of water were injected using a microliter syringe. The tube was shaken vigorously, and a ^{1}H NMR spectrum was recorded. Titration of (OEP)Lu(μ-OH)$_2$Lu(OEP) with H_2O in C_6D_6 and monitoring by ^{1}H NMR spectroscopy gives (OEP)Lu(μ-OH)$_2$(H_2O)$_2$Lu(OEP) after addition of H_2O (1 equiv per Lu). ^{1}H NMR (C_6D_6): δ 9.62 (s, 8 H, CH), 3.80 and 3.74 (m, AB, CH_2), 1.642 ("t", CH_3), −2.2 (br, 6 H, Lu(μ-O*H*·H_2O)$_2$Lu.

(OEP)Y(μ-OH)$_2$Y(OEP) (4b). This was prepared analogously to (OEP)Lu(μ-OH)$_2$Lu(OEP). No yttrium coupling was observed to the O*H* resonance, although it remained sharp. ^{1}H NMR (C_6D_6): δ 9.69 (s, 8 H, CH), 3.99 and 3.93 (m, AB, CH_2), 1.62 ("t", CH_3), −8.18 (s, 2 H, Y–OH). Anal. Calcd for $C_{72}H_{90}Y_2N_8O_2$: C, 67.70; H, 7.10. Found: C, 67.42; H, 7.07.

KMe. The ether solvent in ethereal MeLi was removed under vacuum until the resultant, finely divided white solid achieved constant weight, indicative of complete removal of coordinated ether (ca. 16 h at 25 °C is required). To 0.868 g, 39.5 mmol, of solid MeLi suspended in 120 mL of hexane in a Schlenk tube at 25 °C was slowly added 4.4 g, 39.5 mmol, of KO^{t}Bu as a solid. The suspension was stirred overnight at 25 °C in the drybox. The solution was removed from the drybox and the suspension filtered to give a white powder, which was washed with 3 × 50 mL of hexane to remove LiO^{t}Bu. The white powder was dried under vacuum to give 1.66 g, 78% yield, of KMe. Solid KMe is extremely pyrophoric. No perceptible decomposition is observed (months) at −40 °C under an inert atmosphere. It can be used only in saturated hydrocarbons such as hexane or cyclohexane.

(OEP)Y(μ-Me)$_2$Li(OEt$_2$) (5). A 1.91-mL volume of 1.6 M MeLi was added to 1.26 g, 1.525 mmol, of (OEP)YOC$_6H_3{}^tBu_2$ (**2b**) in 40 mL of ether at −40 °C. This red suspension was allowed to warm to 20 °C and stirred for 3 h. A red powder precipitates during the reaction, which was isolated by centrifugation and washed with 20 mL of ether to afford 0.542 g of (OEP)Y(μ-Me)$_2$Li(OEt$_2$). Yield: 48%. The yield can be improved by combining and concentrating the ether extracts. Yields of up to 82% have been obtained by performing the reaction in ether as above and then adding an equal volume of hexane to assist in precipitating **5**. A ^{1}H NMR spectrum of the residue obtained by removal of the supernatant liquor in vacuum shows only LiOC$_6H_3{}^tBu_2$·OEt$_2$. Anal. Calcd for (OEP)Y(μ-Me)$_2$Li ($C_{38}H_{50}YN_4Li$): C, 69.29; H, 7.65; Y, 13.50; Li, 1.05. Found: C, 65.04; H, 7.66; Y, 14.10; Li, 1.08. Under the conditions used for the elemental analysis, **5** apparently loses coordinated ether. The H, Y, and Li analyses are in excellent agreement, although we have no explanation for the low C analysis.

(OEP)Y(μ-Me)$_2$AlMe$_2$ (6). A 131-μL (2-equiv) amount of $AlMe_3$ was added to a stirred suspension of 0.542 g, 0.74 mmol, of (OEP)Y(μ-Me)$_2$Li(OEt$_2$) in 40 mL of hexane. The reaction is almost instantaneous judging from the rapid dissolution of **5** and the concomitant deep red coloration of the hexane. After 3 h at 20 °C the intense red hexane solution was centrifuged and decanted and the remaining red powder washed with 50 mL of hexane. The hexane was removed under vacuum to afford 246 mg of (OEP)Y(μ-Me)$_2$AlMe$_2$ (**6**) as a red powder. The red hexane insolubles were extracted with 2 × 5 mL of toluene to separate additional (OEP)Y(μ-Me)$_2$AlMe$_2$ from LiAlMe$_4$. A 45-mg amount of white toluene insolubles was isolated (expected theoretical amount of LiAlMe$_4$ is 66 mg). (OEP)Y(μ-Me)$_2$AlMe$_2$ is slightly soluble in hexane, and the combined fractions from above were crystallized at −40 °C from 45 mL hexane to give analytically pure material. ^{1}H NMR (C_7D_8, 25 °C): δ 10.57 (CH), 4.08 and 3.99 [m, CH_2, ABX_3 spin system with J_{AB} = 17 Hz, J_{AX} = J_{BX} = 8.0 Hz (simulated)], 1.87 ("t", Me), −3.72 (AlMe). ^{13}C NMR (C_6D_6, 25 °C): δ 147.68 (CH), 143.98 (CH), 100.94 (C), 20.30 (CH_2), 18.74 (Me), −8.0 (AlMe). ^{13}C NMR (C_7D_8, −60 °C): δ 146.27 (CH), 141.62 (CH), 99.70 (C), *C*H_2 and *Me* resonances obscured by solvent methyl resonance, −8.96 (q, 109.4 Hz, Al*Me*). Anal. Calcd for (OEP)Y(μ-Me)$_2$AlMe$_2$ ($C_{40}H_{56}YN_4Al$): C, 67.78; H, 7.96; Y, 12.54; Al, 3.81. Found: C, 67.54; H, 7.87; Y, 12.45; Al, 3.70.

(OEP)Y(μ-OMe)$_2$AlMe$_2$ (7). A 112-mg sample of (OEP)Y(μ-Me)$_2$AlMe$_2$ was dissolved in 10 mL of hexane and 2 mL of toluene in a small Schlenk tube. This was evacuated and dry O_2 emitted. The solution was stirred for 15 min and the solvent removed under vacuum. There is no trace of (OEP)Y(μ-OH)$_2$Y(OEP) (**4b**) in the crude reaction mixture or of any other product. Recrystallization from toluene/hexane afforded analytically pure (OEP)Y(μ-OMe)$_2$AlMe$_2$. ^{1}H NMR (C_6D_6, 25 °C): δ 10.49 (s, 4 H, CH), 4.00 (m, 16 H, CH_2), 1.85 ("t", 24 H, Me), 0.76 (s, 6 H, O*Me*), −2.23 (s, 6 H, Al*Me*). ^{13}C NMR (C_6D_6, 25 °C): δ 147.44 (CH), 142.52 (CH), 100.37 (C), 46.91 (O*Me*), 20.29 (CH_2), 18.85 (Me), −14.1 (fwhm = 35 Hz, Al*Me*). Anal. Calcd for $C_{40}H_{56}O_2YN_4Al$: C, 64.85; H, 7.62; N, 7.56. Found: C, 64.56; H, 7.40; N, 7.42.

(OEP)Y(μ-^{17}OMe)$_2$AlMe$_2$ (7′). In the drybox, 146 mg, 0.209 mmol, of (OEP)Y(μ-Me)$_2$AlMe$_2$ (**6**) was dissolved in 5 mL of C_6D_6 in a 100-mL Schlenk tube fitted with a septum cap. This was removed to the Schlenk line and 40 mL (1.8 mmol) of $^{17}O_2$ (22% enriched) added with vigorous stirring. After 15 min, the tube was evacuated to remove excess oxygen and returned to the drybox. A ^{1}H NMR spectrum of the solution showed only **7′** and was identical to that for **7**. The C_6D_6 solution was concentrated under vacuum and transfered to a 10-mm NMR tube and the ^{17}O NMR spectrum recorded. ^{17}O NMR (C_6D_6, 22 °C): δ 13.85 ppm (fwhm = 850 Hz).

X-ray Structure Analysis of 1a. A single crystal of **1a** was mounted under nitrogen in a thin-walled glass capillary under nitrogen and held in place using silicone grease. All diffraction experiments were carried out at 200 K on a Nicolet R3m four-circle diffractometer fitted with a LT-1 crystal-cooling device, using graphite-monochromated Mo Kα X-radiation, λ = 0.71069 Å. Unit cell dimensions were determined from 49 centered reflections in the range 16.0° < 2θ < 32.0°. Details of crystal data collection and reduction are given in Table I. A total of 6332 diffracted intensities, including check reflections, were measured in a unique quadrant of reciprocal space for 4.0° < 2θ < 45.0° by Wyckoff ω scans. Three check reflections remeasured after every 100 ordinary

data showed a decay of 5% and a variation of ±2% over the period of data collection; hence, an appropriate correction was applied. Of the 6129 intensity data collected, 5675 unique observations remained after averaging of duplicate and equivalent measurements and deletion of systematic absences, all of which were retained for use in structure solution and refinement. The absorption correction was applied on the basis of the indexed crystal faces, maximum and minimum transmission coefficients being 0.459 and 0.364, respectively. Lorentz and polarization corrections were applied. Structure solution was by conventional heavy-atom (Patterson and difference Fourier) methods and refinement by blocked-cascade full-matrix least squares. Weights w were set equal to $[\sigma_c^2(F_o) + gF_o^2]^{-1}$, where $\sigma_c^2(F_o)$ is the variance in F_o due to counting statistics and $g = 0.0005$ was chosen to minimize the variation in S as a function of $|F_o|$. All non-hydrogen atoms were assigned anisotropic displacement parameters, and all hydrogen atoms, fixed isotropic displacement parameters. All non-hydrogen atoms and the hydrogen atom H(1) were refined without positional constraints. All other hydrogen atoms were constrained to idealized geometries (C-H = 0.96 Å, H-C-H = 109.5°). Final difference electron density maps showed no features outside the range +1.3 to -1.3 e Å^{-3}, the largest of these being close to the lutetium atom. One ethyl group [C(36), C(37a), and C(37b)] showed a two-site disorder, with the methyl carbons well separated and refined as two distinct atomic sites [C(37a) and C(37b)] of occupancy 0.53 (2) and 0.47 (2), respectively. The methylene group [C(36)] was refined as a single atomic site, with some consequent distortion of the apparent geometry around this atom. Residuals at convergence are listed in Table I. All calculations were carried out with Nicolet proprietary software using complex neutral-atom scattering factors taken from ref 50.

Acknowledgment. We thank Prof. Dr. J. W. Buchler (Technische Hochschule, Darmstadt, Germany) for some useful comments.

Supplementary Material Available: Complete tables of data collection parameters, bond distances and angles, anisotropic thermal parameters, and hydrogen atomic coordinates for **1a** (6 pages); a table of observed and calculated structure factor amplitudes for **1a** (21 pages). Ordering information is given on any current masthead page.

Contribution from the Department of Inorganic and Physical Chemistry, Indian Institute of Science, Bangalore 560 012, India

Reactivity of PPh_3 toward $Ru^{II}Ru^{III}Cl(O_2CAr)_4$: Syntheses, Molecular Structures, and Spectroscopic and Electrochemical Properties of $Ru^{II}Ru^{III}(OH_2)Cl(MeCN)(O_2CAr)_4(PPh_3)_2$ and $Ru^{II}_2(OH_2)(MeCN)_2(O_2CAr)_4(PPh_3)_2$

Birinchi K. Das and Akhil R. Chakravarty*

Received December 17, 1990

By the reaction of $Ru_2Cl(O_2CAr)_4$ (**1**) and PPh_3 in MeCN-H_2O the diruthenium(II,III) and diruthenium(II) compounds of the type $Ru_2(OH_2)Cl(MeCN)(O_2CAr)_4(PPh_3)_2$ (**2**) and $Ru_2(OH_2)(MeCN)_2(O_2CAr)_4(PPh_3)_2$ (**3**) were prepared and characterized by analytical, spectral, and electrochemical data (Ar is an aryl group, C_6H_4-*p*-X; X = H, OMe, Me, Cl, NO_2). The molecular structure of $Ru_2(OH_2)Cl(MeCN)(O_2CC_6H_4$-*p*-$OMe)_4(PPh_3)_2$ was determined by X-ray crystallography. Crystal data are as follows: triclinic, $P\bar{1}$, a = 13.538 (5) Å, b = 15.650 (4) Å, c = 18.287 (7) Å, α = 101.39 (3)°, β = 105.99 (4)°, γ = 97.94 (3)°, V = 3574 Å^3, Z = 2. The molecule is asymmetric, and the two ruthenium centers are clearly distinguishable. The Ru^{III}-Ru^{II}, Ru^{III}-(μ-OH_2), and Ru^{II}-(μ-OH_2) distances and the Ru-(μ-OH_2)-Ru angle in [{$Ru^{III}Cl(\eta^1$-$O_2CC_6H_4$-*p*-$OMe)(PPh_3)$}(μ-OH_2)(μ-$O_2CC_6H_4$-*p*-$OMe)_2${$Ru^{II}(MeCN)(\eta^1$-$O_2CC_6H_4$-*p*-$OMe)(PPh_3)$}] are 3.604 (1), 2.127 (8), and 2.141 (10) Å and 115.2 (5)°, respectively. The compounds are paramagnetic and exhibit axial EPR spectra in the polycrystalline form. An intervalence transfer (IT) transition is observed in the range 900-960 nm in chloroform in these class II type trapped mixed-valence species **2**. Compound **2** displays metal-centered one-electron reduction and oxidation processes near -0.4 and +0.6 V (vs SCE), respectively in CH_2Cl_2-TBAP. Compound **2** is unstable in solution phase and disproportionates to (μ-aquo)diruthenium(II) and (μ-oxo)diruthenium(III) complexes. The mechanistic aspects of the core conversion are discussed. The molecular structure of a diruthenium(II) compound, $Ru_2(OH_2)(MeCN)_2(O_2CC_6H_4$-*p*-$NO_2)_4(PPh_3)_2$·1.5$CH_2Cl_2$, was obtained by X-ray crystallography. The compound crystallizes in the space group $P2_1/c$ with a = 23.472 (6) Å, b = 14.303 (3) Å, c = 23.256 (7) Å, β = 101.69 (2)°, V = 7645 Å^3, and Z = 4. The Ru^{II}-Ru^{II} and two Ru^{II}-(μ-OH_2) distances and the Ru^{II}-(μ-OH_2)-Ru^{II} angle in [{(PPh_3)-$(MeCN)(\eta^1$-$O_2CC_6H_4$-*p*-$NO_2)Ru$}$_2$(μ-OH_2)(μ-$O_2CC_6H_4$-*p*-$NO_2)_2$] are 3.712 (1), 2.173 (9), and 2.162 (9) Å and 117.8 (4)°, respectively. In both diruthenium(II,III) and diruthenium(II) compounds, each metal center has three facial ligands of varying π-acidity and the aquo bridges are strongly hydrogen bonded with the η^1-carboxylato facial ligands. The diruthenium(II) compounds are diamagnetic and exhibit characteristic ^{1}H NMR spectra in $CDCl_3$. These compounds display two metal-centered one-electron oxidations near +0.3 and +1.0 V (vs SCE) in CH_2Cl_2-TBAP. The overall reaction between **1** and PPh_3 in MeCN-H_2O through the intermediacy of **2** is of the disproportionation type. The significant role of facial as well as bridging ligands in stabilizing the core structures is observed from electrochemical studies.

Introduction

An interesting aspect of the chemistry of metal-metal multiple-bonded tetracarboxylates is the reactivity of monodentate tertiary phosphines toward the dimetallic cores.[1,2] The usual mode of bonding of the phosphine ligand is axial and/or equatorial with respect to the dimeric core. In these substitution type reactions, the M-M bond order of the core remains unaltered when the dimeric unit is not cleaved. Triarylphosphines are also known[3] to act as three-atom bridging ligands on orthometalation to one aryl group.

Earlier attempts to prepare axially coordinated PPh_3 complexes of ruthenium of the type $[Ru_2(O_2CR)_4(PPh_3)_2]^+$ led to the formation of oxo-bridged diruthenium and triruthenium complexes.[4,5] The reactivity of the diruthenium core is of interest since the dimeric rhodium(II) carboxylates with a similar core structure are known to form stable axial adducts with P- and N-donor ligands.[1,6] The unusual reactivity of the $\{Ru_2(O_2CR)_4^+\}$ core could be due to the stability of its $\sigma^2\pi^4\delta^2(\delta^*\pi^*)^3$ ground electronic

(1) Cotton, F. A.; Walton, R. A. *Multiple Bonds Between Metal Atoms*; John Wiley & Sons: New York, 1982.
(2) Cotton, F. A.; Walton, R. A. *Struct. Bonding (Berlin)* **1985**, *62*, 1.
(3) Chakravarty, A. R.; Cotton, F. A.; Tocher, D. A. *Inorg. Chem.* **1984**, *23*, 4697. Chakravarty, A. R.; Cotton, F. A.; Tocher, D. A.; Tocher, J. H. *Organometallics* **1985**, *4*, 8.
(4) Schröder, M.; Stephenson, T. A. In *Comprehensive Coordination Chemistry*; Wilkinson, G., Gillard, R. D., McCleverty, J. A., Eds.; Pergamon Press: Oxford, England, 1987; Vol. 4, pp 277-518.
(5) Legzdins, P.; Mitchell, R. W.; Rempel, G. L.; Ruddick, J. D.; Wilkinson, G. *J. Chem. Soc., A* **1970**, 3322. Cotton, F. A.; Norman, J. G., Jr. *Inorg. Chim. Acta* **1972**, *6*, 411.
(6) Jardine, F. H.; Sheridan, P. S. In *Comprehensive Coordination Chemistry*; Wilkinson, G., Gillard, R. D., McCleverty, J. A., Eds.; Pergamon Press: Oxford, England, 1987; Vol. 4, pp 901-1096.

0020-1669/91/1330-4978$02.50/0